This document was prepared for the ETI by third parties under contract to the ETI. The ETI is making these documents and data available to the public to inform the debate on low carbon energy innovation and deployment.

Programme Area: Marine

Project: PerAWAT

Title: GH Blockage Modelling Report

Abstract:

This document outlines the issues associated with modelling the effects of bounding surfaces and/or other bodies on the flow field in and around a tidal turbine rotor. A review of the existing literature provides an overview of the available modelling options and also provides a basis for the selection of an appropriate level of model sophistication. The GH Blockage model is described and the rationalised modelling approach is justified. The GH Blockage model uses Potential flow theory to evaluate the effect of bounding surfaces and/or other surrounding turbines on a tidal turbine under investigation. The model is used to predict the three dimensional flow field in and around the tidal turbine, which enables the change in turbine performance to be predicted. The altered flow field around the turbine is also used in modelling the wake mixing and recovery process. A list of key assumptions that the GH Blockage model makes is provided along with the relevant references to existing theory. The method by which the mathematical models are implemented into a working code is described, as is the way in which the GH Blockage model to be incorporated within the GH TidalFarmer Beta code. Flow diagrams of the GH Blockage model algorithms are presented and examples of the outputs are provided.

Context:

The Performance Assessment of Wave and Tidal Array Systems (PerAWaT) project, launched in October 2009 with £8m of ETI investment. The project delivered validated, commercial software tools capable of significantly reducing the levels of uncertainty associated with predicting the energy yield of major wave and tidal stream energy arrays. It also produced information that will help reduce commercial risk of future large scale wave and tidal array developments.

ETI Marine Programme Project
PerAWaT MA1003
WG3WP4 D1 GH BLOCKAGE MODELLING REPORT

Client	**Energy Technologies Institute**
Contact	Geraldine Newton-Cross
Document No	104329/BR/01
Issue	3.0
Classification	Not to be disclosed other than in line with the terms of the Technology Contract
Date	15th June 2010

Author:

M D Thomson / D McCowen

Checked by:

L Gill /J I Whelan

Approved by:

R I Rawlinson-Smith

DISCLAIMER

1.This report is intended for the use of the Client on whose instructions it has been prepared, and who has entered into a written agreement directly with Garrad Hassan & Partners Limited ("GH"). GH's liability to the Client is set out in that agreement. GH shall have no liability to third parties for any use whatsoever without the express written authority of GH. The report may only be reproduced and circulated in accordance with the Document Classification and associated conditions stipulated in this report, and may not be disclosed in any public offering memorandum without the express written consent of GH.

2. This report has been produced from information relating to dates and periods referred to in this report. The report does not imply that any information is not subject to change.

Key To Document Classification

Strictly Confidential	:	Recipients only
Private and Confidential	:	For disclosure to individuals directly concerned within the recipient's organisation
Commercial in Confidence	:	Not to be disclosed outside the recipient's organisation
GHP only	:	Not to be disclosed to non GHP staff
Client's Discretion	:	Distribution at the discretion of AES subject to contractual agreement
Published	:	Available to the general public

Revision History

Issue	Issue Date:	Summary
1.0	12/3/10	Original release – electronic copy only
2.0	04/05/10	Second release, following ETI's feedback from PM2.
3.0	15/06/10	Minor revisions, following ETI's feedback from PM2_final.

Circulation:	Copy No:
ETI	1
GH Bristol	2

Copy No: _____

CONTENTS

EXECUTIVE SUMMARY

This document outlines the issues associated with modelling the effects of bounding surfaces and/or other bodies on the flow field in and around a tidal turbine rotor. A review of the existing literature provides an overview of the available modelling options and also provides a basis for the selection of an appropriate level of model sophistication. The GH Blockage model is described and the rationalised modelling approach is justified.

The GH Blockage model uses Potential flow theory to evaluate the effect of bounding surfaces and/or other surrounding turbines on a tidal turbine under investigation. The model is used to predict the three dimensional flow field in and around the tidal turbine, which enables the change in turbine performance to be predicted. The altered flow field around the turbine is also used in modelling the wake mixing and recovery process.

The GH Blockage modelling theory is described in full with detailed derivations in the main document and in the supporting Appendices. A list of key assumptions that the GH Blockage model makes is provided along with the relevant references to existing theory.

The method by which the mathematical models are implemented into a working code is described, as is the way in which the GH Blockage model to be incorporated within the GH TidalFarmer Beta code. Flow diagrams of the GH Blockage model algorithms are presented and examples of the outputs are provided.

SUMMARY OF NOTATION

Channel characteristics

A	Cross-sectional area (m^2)
b	Width of channel (Diameters)
D_H	Hydraulic radius of the channel (m)
Fr	Froude number (channel)
h	Channel height (Diameters)
b	Channel width (Diameters)
r	Radial distance (m)
z	Vertical height measured from the sea bed or channel floor (m)

Turbine characteristics

C_p	Power coefficient
$C_{pboundless}$ or Cp_b	Power coefficient of the rotor in a boundless flow
C_t	Thrust coefficient
$C_{tboundless}$ or Ct_b	Thrust coefficient of the rotor in a boundless flow
D	Rotor diameter (m)
hh	Turbine hub height (Diameters)
$Re_{turbine}$	Reynolds number across the rotor

Flow Field

a	Induction factor
B	Blockage ratio
E	Specific energy (m^2/s^2)
f	Body forces (per unit volume) acting on the fluid (N/m^3)
g	Gravitational acceleration (m/s^2)
J_0	Bessel function
M	Momentum (Ns)
m	Strength of the source
p	Pressure (N/m^2)
Q	Flow rate (m^3/s)
q	Flow rate (m^3/s)
R	Radius of streamtube (m)
S	Area of the streamtube (m^2)
s_t	Equivalent 2-D turbine diameter (m)
s_0	Width of streamtube upstream (m)
s_2	Width of streamtube downstream (m)
u	Axial velocity component (m/s)
v	Lateral velocity component (m/s)
w	Vertical velocity component (m/s)
U_0	Mean free stream flow speed (m/s)
U_i	Incident flow speed on rotor (m/s)
α	Fractional reduction in velocity downstream in the wake (m/s)
β	Fractional reduction in velocity at the rotor (m/s)
Φ	Velocity potential (m^2/s)
κ	Drag coefficient
ρ	Density (kg/m^3)
τ	Fractional increase in flow speed (m/s)

1-d	one dimension (typically in the x-direction)
2-d	two dimensions
3-d	three dimensions

A general glossary on tidal energy terms was provided as part of WG0 D2 – "Glossary of PerAWaT terms". This is a working document which will be revised as the project progresses.

1 INTRODUCTION

1.1 Scope of this document

This document constitutes the first deliverable (D1) of working group 3, work package 4 (WG3WP4) of the PerAWAT (Performance Assessment of Wave and Tidal Arrays) project funded by the Energy Technologies Institute (ETI). Garrad Hassan (GH) is the sole contributor to this work package. This document describes the theory behind and the method of implementation of the mathematical models used to evaluate the effect of flow blockage on both the performance of and the local flow field around a tidal turbine.

1.2 Purpose of this document

The purpose of WG3WP4 is to develop, validate and document an engineering tool that allows a rapid assessment of the energy yield potential of a tidal turbine array on non-specialist hardware. The specific objective of WG3 WP4 D1 is to both document and provide a technical justification for the use of the existing GH Blockage model within the suite of models that make up the engineering tool: GH TidalFarmer.

1.3 Specific tasks associated with WG3 WP4 D1

WG3WP4 D1 comprises the following aspects:

- A detailed description of the theoretical basis of the GH Blockage model and a technical justification for the rationalised modelling approach.
- A description of modelling methodology.
- A description of the method of integrating the GH Blockage model into the GH complete engineering tool code.

1.4 WG3 WP4 D1 acceptance criteria

The acceptance criteria as stated in Schedule five of the PerAWAT technology contract is as follows:

D1: Blockage modelling report describes:

- The theory and methodology (assumptions and algorithms) behind the blockage /potential flow model

- The method of integrating this model within the Beta code

2 BACKGROUND AND RELEVANT THEORY

This section introduces the concept of flow blockage and the implications of blockage upon a tidal turbine. A review of some relevant theory is provided.

2.1 General description of blockage

Objects within a flow act as an impedance causing the flow to deviate around the object. Blockage effects are generated when bounding surfaces or other objects within the flow restrict the deviation of flow around the object.

The hydrodynamic definition of **Blockage** is:

"The effects of the boundaries on the flow around a body." Maskell (1963).

The flow past a body when bounded by surfaces, such as rigid walls, is subject to blockage. The bounding surfaces prevent free displacement of the flow around the body; hence the local velocities are higher than they would be in an unbounded stream. Hydrodynamic blockage can occur in two distinct forms, wake and solid-body blockage. Solid-body blockage is associated with the volume and shape of the body, and wake blockage is associated with drag on the body, as defined by Maskell (1963).

It is useful to review other relevant definitions:

Blockage correction – A correction made to the results of hydrodynamic experiments conducted in a channel or tunnel of a finite cross-sectional area in order to estimate the equivalent results conducted on the same experimental equipment operating under unbounded conditions. For example corrections made to the results of a resistance experiment in a towing tank in order to estimate the equivalent results in unrestricted water.

Blockage ratio - By defining the Blockage ratio (B) as the swept area of the rotor divided by the relevant cross-sectional area of flow (A), three distinct categories emerge:

1. $B \approx 0$ represents an isolated open turbine, where A is defined as the total flow width multiplied by depth. Even in a relatively narrow channel, the diameter of the turbine is likely to be very much smaller than the width of the channel and hence the blockage ratio will be effectively equal to zero.
2. $0 < B < 1$ is typical of a turbine operating within an array of turbines, where A is defined as the turbine spacing multiplied by the depth. In this case blockage will be due to the effect of the adjacent turbines on each other which is analogous to the effect of walls along their dividing planes on a single turbine.
3. $B \approx 1$ represents the case of a turbine within a duct, where A is defined as the area of the duct and the turbine fills the entire duct (i.e. a hydro-electric turbine and it should be noted that this case will never occur in the Tidal Stream industry).

A body moving through a fluid (or a fluid moving over a body) experiences a drag force, which is usually divided into two components: **frictional drag**, and **pressure drag.**

Frictional drag - arises due to friction between the fluid and the surfaces over which it is flowing. This friction is associated with the development of boundary layers, and it scales with Reynolds number.

Pressure drag - arises due to the eddying motions that are set up in the fluid by the passage of the body. This drag is associated with the formation of a wake and it is usually less

sensitive to Reynolds number than the frictional drag. Pressure drag is important for separated flows, and it is related to the cross-sectional area of the body. When the drag is dominated by pressure drag, the body is defined as a **bluff-body**[1]**.**

Near field – the region around an object defined by a characteristic length scale. Typically the region extends from between one and four length scales. For a rotor the near field is the surround area affected by an adverse the pressure gradient.

A **streamline** is a curve upon which every point is tangent to the velocity field. Streamlines coincide with the paths of a fluid particle when the flow is steady and **u**(x,y,z). The corresponding streamline equations are:

$$\frac{dx}{ds} = u \; \frac{dy}{ds} = v \; \frac{dz}{ds} = w \qquad\qquad ds^2 = dx^2 + dy^2 + dz^2$$

A s**treamtube** is a made up of an infinite number of streamlines so that no mass flux can travel through the side of a streamtube i.e. set of streamlines that form a closed loop. As there is no flow normal to a streamline (by definition) and for a steady, one-dimensional flow the mass-flow rate along a streamtube is constant. In a constant density flow the cross-sectional area of the streamtube gives information on the local velocity.

2.2 General description of a tidal turbine in unbounded flow

The energy in a moving tidal stream is converted into electrical power by a mass of fluid moving over the rotor blades and imparting some of its energy on to the rotor, causing the rotor to turn and drive a generator. For the case of a turbine rotor extracting power from a steady uniform flow, the near field effect can be simply described using the concept of a streamtube. The figure below illustrates the streamtube that encompasses the flow which passes through the rotor swept area and it can be seen that upstream the cross-sectional area is smaller than the rotor swept area. This is because as the flow approaches the rotor it experiences an adverse pressure gradient as a result of the rotor extracting momentum from the flow causing the flow to deflect around the rotor reducing the normal component of flow.. To conserve mass, the cross-sectional area of the streamtube must expand as it approaches the rotor due to the slowing of the fluid. The streamtube continues to expand downstream of the rotor until the pressure gradient reduces to the ambient condition. The fluid that interacts with the turbine blades imparts some of its momentum into a lifting force, which drives the rotor, and in doing so it experiences a change in direction. As Figure 2.1 illustrates the flow starts to rotate slightly in the opposite direction to the rotation of the turbine. As this fluid moves further downstream all the flow within the streamtube eventually moves with the same velocity (αU). The flow outside of the streamtube does not lose any momentum to the turbine, although its velocity will be altered by the presence (and the operating conditions of) the turbine.

.

[1] http://www.princeton.edu/~asmits/Bicycle_web/blunt.html

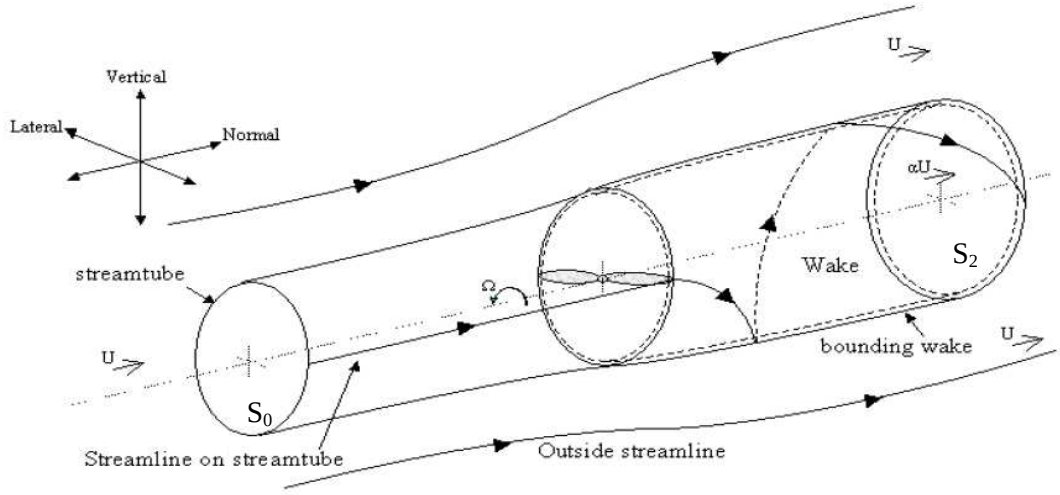

Figure 2.1 The near flow field in and around a rotor in an unbounded flow

The analysis by Thomson (2004) illustrates that 90% of the rotor streamtube expansion occurs within one diameter of the rotor plane. At two diameters from the rotor the wake has expanded to 98% of its final cross-sectional area (i.e. 98% of S_2 downstream) and at three diameters this increases to 99%. Thus for a rotor the near field is typically taken to mean within two rotor diameters up and downstream.

The wake that is generated from the lifting effect on the blades is realised as vortical structures which are trailed and shed from the blades and are bounded from the outer (faster moving) free-stream fluid by the vortices trailed from the blade tips. These trailed vortices convect downstream to form helices. As these vortex helices wrap around themselves to form a tight coil, the downstream wake and the bounding streamtube is formed. Typically the near wake exists for up to one diameter (D) downstream, after which the ambient turbulence in the free-stream flow starts to break down the bounding vortices.

2.3 General description of blockage effects on a tidal turbine

A turbine can be considered to be similar to a bluff-body at certain operating states (despite being effectively porous) because it has a significant wake flow. This situation can give rise to both wake and solid-body blockage. However, the axial length of a rotor is insignificant relative to its diameter and therefore its solid-body blockage will be minimal. Thus when a rotor is placed within a confined flow, the flow outside the rotor streamtube will be travelling at an increased speed compared with that in an unbounded flow. The introduction of other effects around a tidal turbine, i.e. flows induced by other bodies or surfaces, will have an effect on the rotor streamtube causing it to deform from the axisymmetric shape shown in Figure 2.1 above. Changes in the streamtube cross-sectional area will change the performance and loading experienced by the rotor compared to the unbounded flow.

To provide an indication of the potential impact that bounding surfaces might have on the flow in and around the tidal turbine rotor the flow around an unbounded rotor can be reviewed (Thomson, 2004). Any flow moving towards a bounding surface will be re-directed into the stream-wise direction. Figure 2.2 below shows the magnitude of the perpendicular velocity component (i.e. that parallel to the rotor plane) as a function of the distance away from the rotor (the blue line describes the distance from the rotor centreline, where as the yellow line describes the distance from the rotor to blade tip). At a distance of 1.5D (3R) from the turbine centreline the perpendicular flow speed is 1% of the mean flow speed (in the

normal direction). The impact redirecting some flow in to the stream-wise direction causes an overall increase in the flow in the normal direction and thus an increase in flow through the rotor swept area.

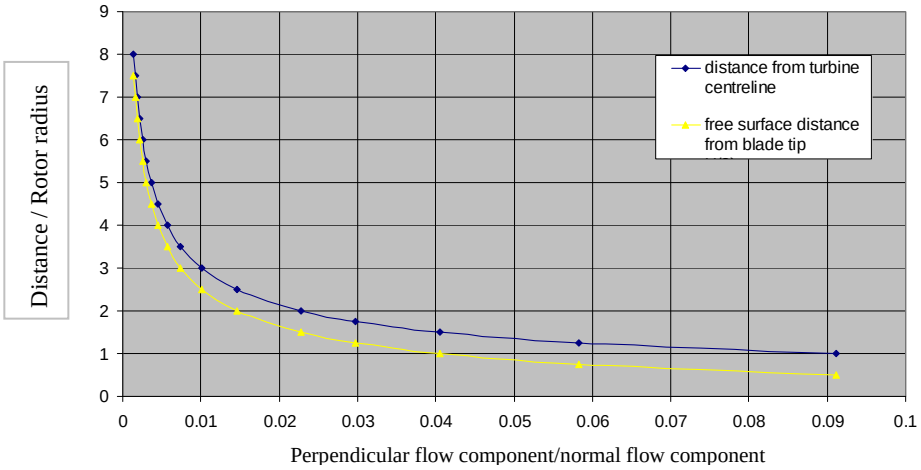

Figure 2.2 Perpendicular flow in the plane of the rotor at varying distances away from the turbine centreline in unbounded flow

As shown in the above figure, at distances greater than 1.5D the effect is considered to be small, however, for distances similar or less than this it is expected the increase in flow through the rotor swept area will have an appreciable effect on rotor performance and loading.

The areas for commercial scale deployment of tidal arrays are typically where the water depth is between 30 – 100 metres. The desire to maximise energy capture means that the swept area of the tidal turbine will be at a practical maximum resulting in non-dimensional depth of 1.5-5D. At these smaller depths there is likely to be a certain amount of flow blockage generated between the sea bed and the free surface.

For viable commercial energy generation tidal turbines will need to be deployed in large arrays where infrastructure economies of scale can be realised. Typical commercial-sized farms are expected to be of the same rated power order of magnitude as offshore wind farms i.e. 100s of MWs. The implication of this and the nature of bi-directional tidal flows means it is likely that the lateral spacing between turbines will be minimised, within practical installation and site specific seabed conditions constraints. Marine Current Turbine's SeaGen turbine has a lateral spacing of 1.5D between the twin rotor centres (i.e. a gap of 0.5D). Thus the expected range for lateral spacings between adjacent devices could also be between 1.5D -5D.

Together vertical and lateral bounding effects increase the potential blockage effect to a level which could have appreciably affect on turbine performance. Thus it is considered important to quantify these effects.

Various studies have been conducted into the effects of blockage on turbines and bluff-bodies (Maskell, 1963), and developed to consider the free-surface, e.g. Scott (1976), Bai (1979), Durgun & Kafali (1991), Whelan (2009). As mentioned earlier, the presence of bounding surfaces acts to re-direct the vertical and lateral components of the flow into the stream-wise direction, causing an overall increase in the flow through the swept area of the turbine. This leads to:

- increased torque or rotor speed (depending on the rotor control strategy),
- increased loading experienced by the turbine,
- potentially, increased power capture
- and, an altered flow field around the rotor

The last point impacts on wake recovery and expansion. As the flow velocity in the bypass region around the turbine (and hence the wake) will be increased due to the restriction of bounding surfaces the resulting wake flow field, when compared with the same rotor operating in an unbounded flow, will be different. This in turn will have an impact on the rate of wake mixing and recovery. Hence when evaluating array performance and inter-array flow effects both the change in rotor performance and the alteration to the local flow field will need to be evaluated.

2.4 A review of existing modelling methods

A review of the literature reveals an extensive body of theory which can be adopted from both wind energy and naval propulsion sciences. However, to date research into the analysis of the effect of the bounding free surface and seabed on tidal turbine rotors has been limited. The following section provides a review of the relevant literature and applicable theories.

Outlined below are the four main theories associated with evaluating turbine performance. Further description of the modelling method and the ability to represent the blockage effects is given in the following sub-sections:

- Actuator disc theory
- Blade element momentum (BEM) theory
- 3-d Potential flow methods
- Computational Fluid Dynamics (CFD)

2.4.1 Actuator disc model in boundless flow

Propeller theory was developed by Betz (1920), using classical analysis. Based on an ideal fluid and an ideal rotor (disc), a momentum integral is taken over a near field control volume to correlate the turbine performance to the reduction in flow speed in the wake or the expansion of the wake. The rotor performance must be evaluated taking into account the viscous properties of the rotor blade via, for example, a BEM code. Thus this theory only yields the relationship between the flow speeds in the streamtube to the performance of the rotor (Cp, the coefficient of power). It does not predict the flow field outside of the streamtube.

Actuator disc theory reduces the problem to a linear one-dimensional system and simplifies the action of a turbine by representing the rotor as a disc with an infinite number of blades. The theory is based upon the following assumptions:

1. Homogeneous, incompressible, steady fluid flow
2. Uniform thrust over the disc with no frictional (drag) losses

3. Static pressure in the far field (i.e. the pressure is the same far upstream as it is far downstream)
4. No rotation imparted into the flow due to the rotating blades

By simulating the rotor as a disc with an infinite number of blades a pressure jump across the disc is created without making an immediate change in velocity. This pressure jump represents a reduction in momentum, which results in the fluid within the streamtube slowing down in the wake. The result of this retardation is that the streamtube's cross-sectional area expands and the flow inside the streamtube far downstream is much slower than that of the flow outside of the streamtube, as illustrated below:

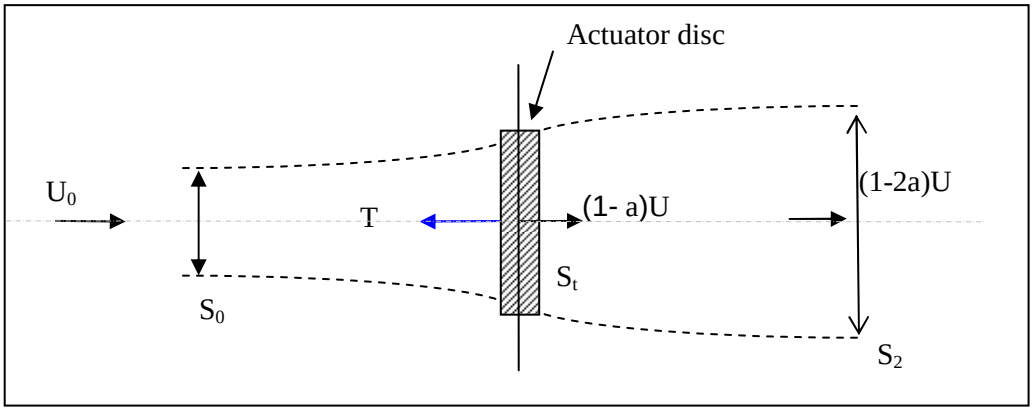

Figure 2.3 Perpendicular flow in the plane of the rotor at varying distances away from the turbine centreline

Actuator disc theory is reviewed in many textbooks on helicopter and rotor aerodynamics (e.g. Wilson & Lissaman 1974). Actuator disc theory characterises the flow in the wake as a function of the operating thrust and power:

$$Ct = \left(1-\alpha^2\right) = 4\cdot\left(\beta-\beta^2\right) = 4\cdot a\cdot\left(1-a\right)$$

and

$$Cp = \tfrac{1}{2}\left(1-\alpha^2\right)\cdot\left(1+\alpha\right) = 4\cdot\left(\beta^2-\beta^3\right) = 4\cdot a\cdot\left(1-a\right)^2$$

where β and α are the fractional reductions in velocity at the rotor and downstream in the wake, respectively. β and α can be represented in terms of the induction factor, a, as:

$$\beta = (1 - a)$$

$$\alpha = (1 - 2.a)$$

The plot below shows the relationship between flow within the streamtube and the rotor power and thrust.

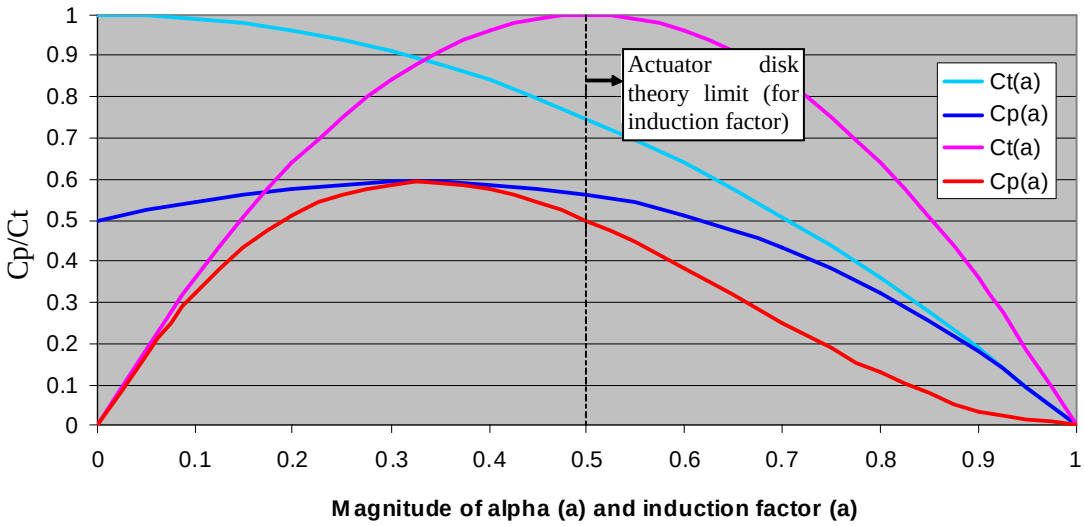

Figure 2.4 Boundless Actuator disc characteristics

In order to evaluate the boundless efficiency of propellers tested in a wind tunnel Glauert (1933) derived an iterative method based on a momentum balance to determine the equivalent free-stream speed required to produce the same thrust at the rotor as occurs in the tunnel. These and other correction methods are comprehensively summarised in both Rae & Pope (1984) and the AGARD publication edited by Ewald (1998). Blockage corrections have traditionally been developed to evaluate the equivalent conditions in unbounded flow. The following sub-sections describe different approaches for the development of correction factors for different types of 'blocked' flow.

2.4.2 Actuator disc theory applied to flow in a tunnel

Mikkelsen (2003) looked in detail at actuator disc methods applied to wind turbines. He proposed an axisymmetric correction factor for the tunnel blockage effect on a rotor by modelling the rotor as an actuator disc and performing an axial momentum balance, which compares well to the approximate solutions of Glauert (1933).

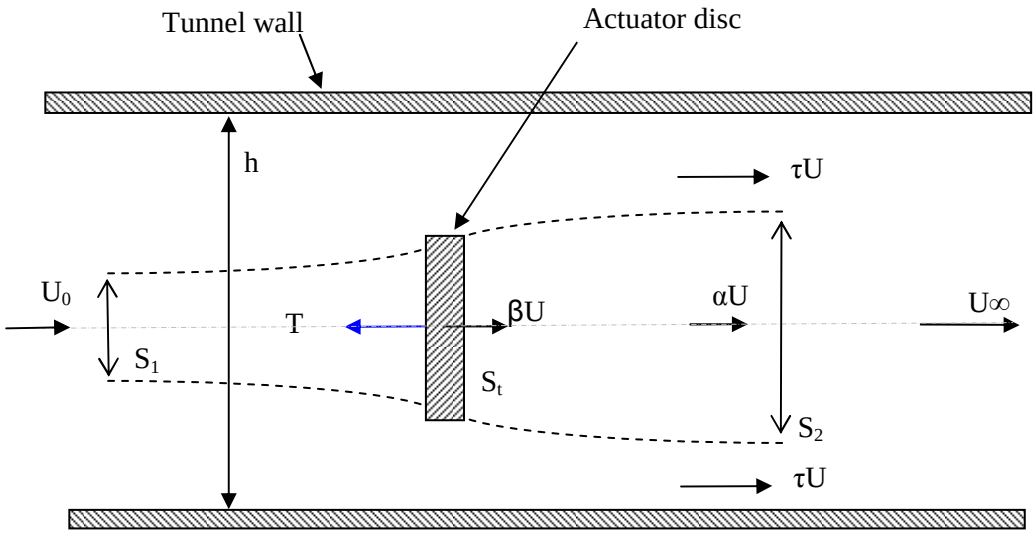

Figure 2.5 Schematic of an actuator disc in tunnel flow

The figure above shows that flow around the rotor streamtube accelerates to a flow speed greater than the upstream flow, where τ is the fractional increase in flow speed (note $\tau > 1$). Garrett & Cummins (2007) developed a 1-d actuator disc analysis which considers turbine flows constrained between (rigid) side walls, in order to assess the efficiency of tidal turbines, Whelan (2009) went on to derive the following expression for τ:

$$\tau = \frac{1-\alpha + \sqrt{B - 2\alpha B + \alpha^2 (1 - B + B^2)}}{1-B}$$

Where B is the Blockage ratio of the rotor swept area to the tunnel cross section. For a given α and β, Whelan (2009) showed that Cp and Ct can be evaluated using the following formulas:

$$Ct = \tau^2 - \alpha^2$$

$$Cp = \beta \cdot Ct$$

So for a given wake flow and blockage ratio, the rotor thrust and power can be evaluated.

This solution is applicable to the 3-d situation provides there is symmetry along the rotor centreline in the lateral and vertical planes.

2.4.3 Actuator disc theory applied to flow in a channel

The free surface is a dynamic boundary which means changes in the flow field may impact on the position of the free surface in both space and time. Adverse pressure gradients in front of a rotor, or its support structure, may cause a local increase in free surface elevation, leading to an unsteady free-surface wave propagating away from the rotor. These time varying effects could impact on wake form stability, which could lead to changes in power performance. The extent of the free-surface disturbance is governed by the disturbance Froude number. For typical full scale real site flow speeds and expected rotor length scales,

the Froude numbers are very low, suggesting the surface waves will be small in comparison with the wake form.

The impact of removing momentum from a channel has been studied in great depth by hydraulic scientists and engineers. The presence of a free surface means that any change in the momentum of channel flow will result in a change in the surface elevation. Channel flows with Froude numbers of less than unity experience a reduction in downstream flow surface elevation coupled with an increase in mean flow speed as shown in the figure below (further detailed proofs are given in Appendix A). Whelan (2009) has developed the actuator disc theory of Garrett and Cummins (2007) to incorporate these free-surface changes, which reduces to the above equation for τ when the Froude number tends to zero. In both cases the axisymmetry of the solution (compared to the unbounded) is lost due to the introduction of a deforming free surface, thus the solution is only valid in cases where a 2-d solution matches the Blockage ratio 0< B < 1 i.e. case 2 as described in Section 2.1 (i.e. where the rotor area is smeared over the width of the channel).

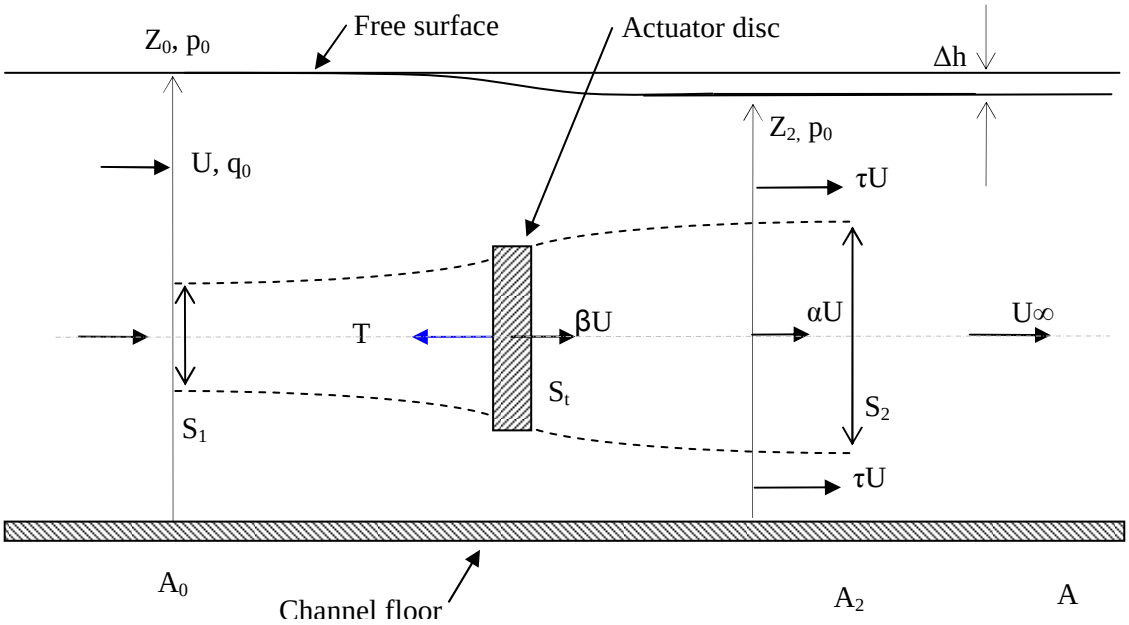

Figure 2.6 Schematic of an actuator disc in channel flow

The 1-d momentum balance across the channel is described by

$$F = \int_0^{z1} (p_a + pgz)dz - \int_0^{z2} (p_a + pgz)dz - p_a(z_0 - z_2) - p(z_2 - s_w)(\tau U)^2 - \rho s_w(\alpha U)^2 + pz_0U^2$$

$$= \frac{1}{2}\rho g\left(2z_0\delta z - (\delta z)^2\right) + \rho U^2 z_0(1-\tau) + \rho\beta U^2 s_t(\tau - \alpha)$$

As shown by Whelan (2009), this yields a quartic equation in τ(α, Fr, B)

$$Fr\tau^4 + 4\alpha Fr\tau^3 + (4B - 4 - 2Fr)\tau^2 + (8 - 8\alpha - 4Fr\alpha)\tau + (8\alpha - 4 + Fr - 4\alpha^2 B) = 0$$

There are four solutions to this equation which must be understood in order to select the correct (physical) solution and to understand the limits of this theory. The figure below shows an example of the four different solutions as a function of the velocity in the far wake

(α) where the Froude number is 0.14 and the Blockage ratios is 0.64. It can be seen that only one solution provides a physically meaningful answer, such that when α is 1, τ is also 1. Where the subcritical and supercritical solutions meet the solution becomes complex, suggesting that there is a limit to the amount of wake retardation for a particular set of flow condition.

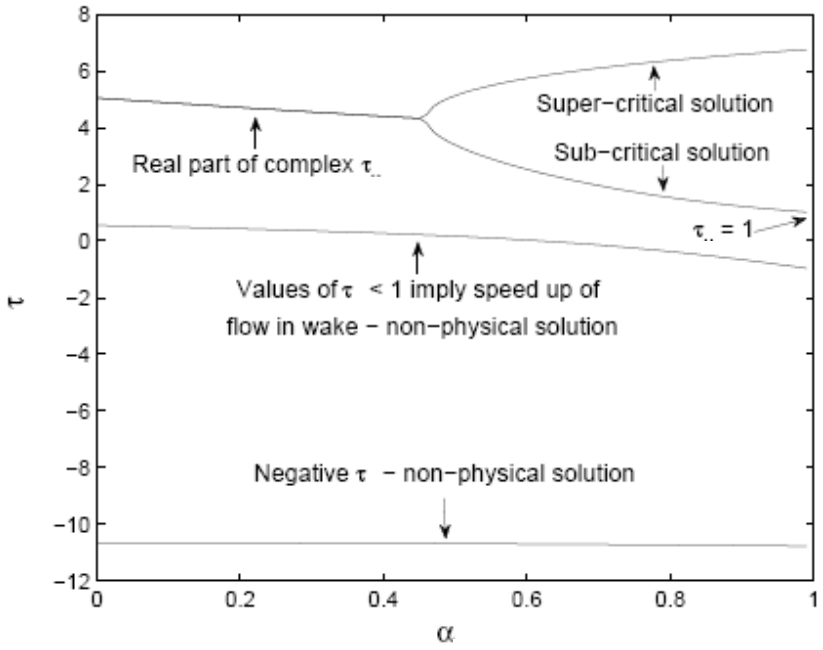

Figure 2.7 Solutions to the quartic equation [Whelan (2009)]

Again the following formulas are used to evaluate the altered Ct and Cp.

$$Ct = \tau^2 - \alpha^2$$

$$Cp = \beta \cdot Ct$$

2.4.4 Blade Element Momentum (BEM) theory

Blade Element Momentum (BEM) theory is the most widely adopted method for the calculation of loads on wind turbines, and hence in the design of wind turbines. Some examples of its use include Garrad Hassan's 'GH Bladed' (Bossanyi, 2007) and the 'AeroDyn' code developed by Laino (2005). Both of these codes have been extensively validated against measurements and have been shown to give good agreement. BEM theory is based on one-dimensional actuator disc (or momentum) theory and sectional blade element theory (described in detail in Burton et al. 2001). Tidal turbine developers such as Marine Current Turbines Limited (MCT) and Tidal Generation Limited (TGL) have adopted BEM codes for loading and performance predictions.

The specific rotor blade geometry is required to conduct a blade analysis of the hydrodynamic forces produced as the fluid flows over an element of the blade. Integrating over the blade elements yields the total thrust and torque produced by the rotor. The effects

of viscosity are empirically incorporated into the model through the blade section data (CL and CD), and hence the accuracy of a BEM simulation is clearly dependent on the quality of the input data, as discussed by Tangler (2002). Given a rotor geometry, hydrofoil characteristics a rotational speed and a flow speed the value of Cp can be found.

The BEM approach is adopted due to the relative simplicity of its computational implementation and because it has been applied very successfully to both horizontal and vertical axis wind turbines in unconstrained flows. Three-dimensional effects that occur in reality cannot be fully accounted for using the simple BEM approach alone, such as the vortices that trail from both the tips and roots of the rotor blades. But corrections can be used (described in Prandtl & Tietjens (1957)) to account for the losses due to these trailing vortices. Blockage effects (such as the presence of the ground) have been normally ignored to date. Actuator disc theory corrected for tunnel or channel flow could be utilised within a BEM code as a correction factor, thus accounting for the presence of the free surface. But the theory does not evaluate the change in the surrounding flow field.

2.4.5 3-d Potential flow methods

Potential flow methods idealise the fluid to allow analytical solutions of the flow field around a body (such as a turbine) to be found. They vary in computational intensity from simple potential models in which the body is represented by a source or sink, to vortex wake models (panel methods and unsteady rotor lattice methods), which employ lifting line or surface theory to represent a body(s) in a flow e.g. a collection of sources or point vortices. The velocity at any point in the domain due to the distribution of sources, sink or vortices is then evaluated from Potential flow theory, e.g. the Biot-Savart law. N.B. The various actuator disc methods discussed in the previous sections assume inviscid, incompressible and irrotation flow (i.e. potential) flow, but are not defined here as a potential flow method.

The aerospace industry has used panel methods extensively in the design of aerodynamic structures due to their rapid, compared to full CFD, computational time. The assumption of an ideal fluid is fair given the very high Reynolds numbers in which the rotor is operating, but the major drawback is the inability to deal directly with viscous effects (boundary layers and flow separation). Many researchers have modelled wind turbines wakes and now tidal turbines wakes (Li, 2007) successfully using this method. Potential theory offers a well-proven, very robust and computationally-efficient approximation of the flow field.

The fixed wake method and free-wake method are the two predominant vortex methods in wind turbine numerical methods. In addition, there are some special modifications or hybrid methods. The vortex methods were initially developed to evaluate the performance predictions of rotors operating in a boundless flow. Force, torque and power are determined by the Kutta-Joukowski law and local circulations, as described in Newman (1977) in the application to marine propellers. The fixed wake model in a uniform flow will simply move unaltered downstream with the advancement of the tidal stream, whereas in the free wake model the wake interacts with itself as the solution is stepped forward in time. Wang & Coton (2000) used a prescribed wake low-order panel method to investigate wall effects on wind turbine wake flows and much effort has been expended by ship sciences modelling the effect of free-surface disturbance of a submerged propeller, e.g. Breslin and Andersen (1994). In general these models have not received as wide attention as the less computationally intensive 1-d actuator disc and BEM methods, mainly due to the complex set-up requirements. They are, however, much more computationally efficient than a full Navier Stokes flow solver.

Recently vortex particle methods have been employed for determining the performance of the flow field around tidal turbines, for instance Li & Calisal (2007) have built on the discrete vortex method with a free wake for a vertical-axis turbine originally developed by Strickland et al. (1979) and have found good agreement with Strickland's measurements in a towing tank. SuperGen Marine has been developing a Potential flow model to investigate free surface effects (Topper, in progress). The purpose of this research is to evaluate the free-surface disturbances created by close proximity of the device to the free-surface. No texts have been published on this work, though the author is presently writing-up his thesis. It is understood that model developed is limited in its application and requires further improvements before it could be used by others for research purposes.

The GH method will employ Potential flow theory, however it does not utilise any of the vortex methods described above. See Section 3 for details of how Potential flow theory is employed in the GH Blockage model.

2.4.6 Computational Fluid Dynamics (CFD)

CFD numerically solves either simplified or the full Navier-Stokes (NS) equations; typically this requires millions of calculations to solve the equations of motion for each node on the discretised spatial flow domain (i.e. the grid). Even with high-speed supercomputers only approximate solutions can be achieved in many cases. Fully viscous CFD simulations are not used in the wind energy industry for day-to-day design purposes due to the intensive nature of re-meshing design alterations, as well as the high computational power requirements. A lack of reliable turbulence models is also a factor preventing their use for full design purposes. However; CFD methods are useful for more detailed investigations, such as looking at the effects of complex rotor geometry.

It is possible to numerically solve the Navier-Stokes non-linear Partial Differential Equations (PDE's) directly for laminar and turbulent flows when all of the relevant length scales can be resolved by the grid i.e. Direct Numerical Simulation (DNS). In general; however, turbulent flow produces fluid interaction at a large range of length scales limiting DNS to low Reynolds number flow (<= 4000), even on supercomputers.

For most applications at higher Reynolds numbers the turbulent flow regime is accounted for by modifying the Navier–Stokes equations to include a turbulence model. The two most common approaches are Large Eddy Simulations (LES) or Simulated Eddy Models (SEM) and the Reynolds-averaged Navier–Stokes equations (RANS) formulation, with the k-ε model or the Reynolds stress model.

Reynolds-averaged Navier–Stokes (RANS) equations are the oldest approach to turbulence modeling (an example of a commercial package is Fluent). It is a common misconception that the RANS equations do not apply to flows with a time-varying mean flow because these equations are 'time-averaged'. In fact, statistically unsteady (or non-stationary) flows can equally be treated. This is sometimes referred to as URANS.

To numerically solve the selected model a discretisation method can be used. Some common methods include:

- Finite volume method (FVM) which is the ‘classical’ approach used most often in commercial software and research codes, but which has problems with unstructured meshes.

- Finite element method (FEM). This method is popular for structural analysis of solids, but is also applicable to fluids. The FEM formulation requires special care; however, to ensure a conservative solution.
- Finite difference method. Is simple to program, but it is currently only used in few specialised codes. Modern finite difference codes make use of an embedded boundary for handling complex geometries, making these codes highly efficient and accurate.

The basic CFD methodology follows a basic procedure.

- Pre-processing
  - The geometry (physical bounds) of the problem is defined.
  - The domain occupied by the fluid is divided into discrete cells (the mesh). The mesh may be uniform or non-uniform.
  - The physical modeling is defined – a system of equations in discretised form
  - Boundary conditions are defined. This involves specifying the fluid behavior and properties at the boundaries of the problem. For transient problems, the initial conditions are also defined.
- The simulation is started and the equations are solved iteratively as a steady-state or transient problem.

These models all rely on expert users, especially when incorporating flexible boundary conditions such as a free surface.

In the wind industry the unsteady incompressible Navier-Stokes solver EllipSys3D (developed by Riso and DNU) was used by Zahle et al. (2007) to model the rotor-tower interaction. The EllipSys3D code is based on the RANS method, has the equations formulated in the turbine plane of reference and uses the so-called k-w turbulence model. In a review of wind turbine aerodynamics, Snel (2003) gives further detail on this code and other similar viscous methods adopted within the industry. CFD simulations incorporating a simplified model of the turbine have been widely used to investigate various effects on turbines. Antheaume et al. (2008) have simulated various blocked conditions using a Navier-Stokes computation of the outer flow field coupled with a description of the inner flow field provided by experimental results from a Darrieus vertical axis turbine.

Recently there has been much activity in using CFD to model tidal turbines, however in the majority of this work the rotor has been represented as a porous disc. O'Doherty et al (2009) and Gretton et al. (2006) both used commercial packages to predict the performance of the both horizontal and vertical axis rotors. Others have used CFD to model the wake recovery process. Gant & Stallard (2008) used CFD to investigate the effects of turbulence in tidal flows on the wake structure by modelling the turbine as a porous plate. Their results indicate that the wake is shorter in the presence of large coherent turbulent structures compared with the length of the wake in steady flow. Others, including Bai (2009), Harrison (2009), Blunden et al. (2009) have also used porous discs or plates to represent turbines or row of turbines in an array. In most cases RANS k-w turbulence models are used.

As yet no one has looked at the effect of the free-surface on performance and loading using CFD.

2.4.7 Application to ducted and open-centre rotors

Within the PerAWAT project three fundamental rotor configurations have been selected for analysis:

- Three bladed horizontal axis axial flow turbine (three bladed turbine)

- Ducted horizontal axis axial flow turbine (ducted turbine)
- Open-centre horizontal axis axial flow turbine (open-centre turbine)

The majority of the simpler axisymmetric models for ducted turbines in the literature require additional input usually taking the form of an experimental correction or using heuristic arguments to allow complete calculation of the performance of the turbine. Actuator disc theory is applicable to many configurations of rotor (horizontal axis (HA) or vertical axis (VA)) as it is concerned only with the extraction of linear momentum. The introduction of a finite duct induces flow augmentation, the extent of which is a function of the duct geometry and the operating state of the rotor. Both Jamieson (2008) and van Bussel (1999) have used momentum methods to investigate the performance of ducted (wind) turbines. Jamieson's corrections have been validated with CFD and implemented into standard blade element theory (GH Tidal Bladed).

The analysis of van Bussel shows that the linear-cube relationship for flow speed to power is not applicable in the case of the ducted turbine because a significant back pressure results at the exit of the duct. The addition of flow constriction from the bounding surface will further add to the flow augmentation, and potentially change the optimum duct/rotor configuration. Although the rotor operating point can be changed to better match the changed duct/rotor configuration, ducts usually have fixed geometry. Hence the use of simpler models may be insufficient to evaluate performance changes due to bounding surfaces. A similar problem occurs with the open-centre device. The balance of flow through the open centre to the rotor will be changed by blockage effects, potentially changing the optimum hole/rotor configuration and thus generating a more complicated interaction.

So although it is likely that all three concepts will be affected by blockage, it is not clear that the simpler methods will be applicable to the ducted and open-centre configurations. Although actuator disc theory (and the correction of it to tunnel and channel flow) is directly applicable to a ducted and open-centre turbine (the duct itself is subject the Betz limit) the relationship between blockage and performance enhancement is likely to be more complex and thus experimental and numerical investigations are required to further explore these relationships.

2.4.8 Summary of existing theory

Actuator disc theory is based on the assumption of an ideal fluid and can be used to correlate the performance of a turbine to the amount of expansion in the wake, but it does not predict the flow field around the turbine. Corrections to account for blockage due to the effects of bounding surfaces have been developed, but often in real flows the axisymmetric assumption breaks down. Fraenkel (2006) has attributed the enhancement in performance over that predicted by a BEM model of MCT's isolated un-ducted horizontal-axis turbine Seaflow (the predecessor of SeaGen) largely to blockage. This suggests that it will be important to model the 3-d flow field around the rotor and incorporate the potential effects of blockage on performance. Even if this only equates to an average increase of 1 or 2% in performance, it still could represent a significant increase in farm annual energy yield.

BEM theory does not solve the flow domain and thus can not be used to directly predict the changes in performance due to bounding surface and /or other rotors.

Both Vortex methods and CFD are useful methods in the investigation of blockage on rotor performance and near field wake structure. As part of the PerAWAT project several CFD models will be developed and used to investigate the impact of blockage on rotor

performance and near field wake structure. These results will inform the GH Blockage model, but their complexity precludes their direct use in an engineering tool.

Table 2.1 Summary table comparing modelling methods

Existing model	Advantage	Disadvantage
Actuator disc theory	Simple model. Proven method (high correlation to measurements) for tunnel testing.	Limited to 2D scenarios. Does not predict any flow acceleration outside of the streamtube.
Blade element momentum (BEM) theory	Relatively simple model. Proven method to predict induction factors (high correlation to measurements)	Does not easily incorporate the effect of bounding surface (external model required). Does not predict any flow acceleration outside of the streamtube.
3-d Potential flow methods	Proven method in the wind industry (good correlation to wind tunnel experiments). Potential theory allows for inclusion of bounding surfaces (including the free-surface)	Relatively complex to set up. Not insignificant computational effort. Representation of the seabed and free-surface is possible, but computational effort is increased. Inviscid approach, thus requires a form of correction for incorporation of viscous effects.
Computational Fluid Dynamics (RANS)	Solves the fundamental equations to the higher order.	Very sensitive to set-up (selection of most appropriate turbulence model etc.). Models require device specific calibration i.e. a detailed geometric description in order to gain the required accuracy from the solution. RANS models using a porous disc representation of a rotor are unproven when looking at changes in performance due to blockage. Very computationally expensive.

3 THE GH BLOCKAGE MODEL

This section introduces the GH Blockage model and the reasoning behind it.

The purpose of the GH Blockage modelling is twofold: firstly to predict the change in turbine performance (Cp & Ct) due to constraining boundaries and secondly to predict the altered flow field around the turbine which may impact on the wake recovery and/or other turbines.

3.1 GH modelling philosophy

GH's modelling philosophy is to provide engineering solutions to meet a commercial need, and in the case of tidal array design this means providing a design tool that can offer practical solutions to aid the iterative design process. To develop an appropriate design tool, rationalised modelling methods based on a physical understanding of the Navier-Stokes (NS) equations that provide robust estimates with known uncertainties are preferred to more complex numerical methods.

3.2 Description of the GH Blockage model

The GH Blockage model uses Potential theory to simulate the flow field around a turbine's expanding streamtube. A simplified mathematical description of a rotor operating in a uniform flow is used to predict the shape of the streamtube. Additional rotors can be added, as can a representation of bounding surfaces. The change in streamtube shape induced by the other rotors or bounding surfaces is used to predict an altered operating state and an iteration method is employed to converge on a solution which satisfies physical characteristics of the operating rotor. For the converged solution the change in performance is evaluated by measuring the change in streamtube shape. The parameters evaluated via this process are then used to evaluate the flow field around the rotor for the purpose of wake modelling.

3.3 Justification for the rationalised modelling approach

The aim of the GH Blockage model is to calculate changes in rotor performance and predict the flow acceleration around the rotor streamtube. To estimate the potential change in performance the modified actuator disc theory can be used as a rough guide, but it cannot model 3-d asymmetric effects such as adjacent rotors operating at a slightly different height and in a different plane to the rotor of interest. Actuator disc and BEM methods do not model the flow field around the rotor and are of limited use for the purpose of the GH tool. In comparison CFD and vortex lattice methods can be used to model the detailed effect of changing the flow direction onto a specific blade geometry. However, both are too computationally intensive for the purpose of an array design tool. Typically CFD is used at the validation stage of a design, or when better understanding of complex fluid/structure interaction is required. Evaluating the array flow field using CFD to model each rotor is a hugely complex and very computationally expensive task. CFD modellers have looked at simplifying the computation by representing the rotor as a porous disc (as done by Gant & Stallard (2008)) or strip, but even then the computations are onerous and not feasible for an array design tool requiring wake calculations for numerous different operating states (e.g. flow speeds) and layout configurations. For these reasons GH believes that full CFD should be reserved for design validation of rationalised numerical methods.

The table below highlights the change in order of magnitude of computational effort with modelling an increased definition of the rotor. Although the most simple of Vortex methods

might be computationally feasible, the practical process of setting-up the model makes this method unattractive for an array design tool.

Table 3.1 Typical computation times source [Li (2007)]

Method	Time[s]
Actuator disc (theoretical)	1
Potential flow – simple*	10
Vortex method (fixed-wake)	100
Vortex method (free-wake 2D)	1e4
Vortex method (free-wake 3D)	1e5
CFD – RANS (Fluent) 2D	1e6
CFD – RANS (Fluent) 3D	>>1e6

*The GH Blockage model uses Potential theory to simulate the flow field around a turbine's expanding streamtube. However, the rotor is represented by a simple source term i.e. a single mathematical term compared to a detailed matrix of terms used in the Vortex methods. This simplification has the advantage of yielding a much more efficient computation which is independent of the specific rotor configuration. The main disadvantage is that it does not model the flow within the streamtube and thus cannot directly predict rotor performance. This, however, is not essential. The standard approach in the wind industry is to use rotor characteristics defined by the turbine manufacturer and certified by an independent body. The same approach is also valid here, except that the standard power and thrust curves will be altered due to bounding effects and thus there is a need to evaluate the site specific blockage. So instead of predicting the absolute performance characteristics the aim is to predict the change performance due to bounding effects.

Using Potential theory allows the model to be developed with the use of additional functions to better represent the specific site conditions. Additionally, as a well-established modelling approach there is a wealth of expertise and active developments in the mathematical functions available for adoption. Another major advantage to using Potential theory is the ability to directly solve specific points in the flow field (as compared to solving the total flow domain many times until the solution converges), thus computations can be limited to the specific area of interest.

4 GH BLOCKAGE MODEL THEORY

This section describes the theory behind the GH Blockage model. The following section provides an introduction.

4.1 The basics

The flow field generated by a turbine and its surroundings is governed by the fundamentals of fluid dynamics. To model a flow field the equations which govern fluid motion must be solved using the relevant boundary conditions. There are many introductory texts on the subject, e.g. Paterson (1983), Lighthill (1986), Massey (1989), but a short review is presented here:

The application of the conservation of linear momentum (i.e. Newton's Second Law of Motion) together with the assumption that the fluid stress is the sum of a diffusing viscous term plus a pressure term, coupled with the continuum assumption, leads to the Navier-Stokes equations.

The Navier-Stokes equations are a set of non-linear partial differential equations that describe the velocity field or flow field of the fluid at a given point in space and time. The non-simplified equations do not have a general closed-form solution, thus must be solved numerically and with the introduction of a turbulence model or simplified in a way that allows them to be solved.

$$\rho\left(\frac{\partial \mathbf{u}}{\partial t} + \mathbf{u}\cdot\nabla\mathbf{u}\right) = -\nabla p + \nabla\cdot\mathbf{T} + \mathbf{f}$$

where **u** is the flow velocity, ρ is the fluid density, p is the pressure, **T** is the stress tensor, and **f** represents body forces (per unit volume) acting on the fluid.

The mass conservation equation can be reduced to the continuity equation for incompressible fluids, and because no mass is created or destroyed in the system, the standard continuity equation is derived.

$$\nabla\cdot\mathbf{u} = 0$$

Ignoring the effects of viscosity, Euler derived the following equation of motion for a fluid as:

$$\rho\frac{\partial \mathbf{u}}{\partial t} + \rho(\mathbf{u}\cdot\nabla\mathbf{u}) + \nabla p = \mathbf{f}$$

The Euler equation can be simplified further if an irrotational velocity field is assumed. This allows the velocity field to be described as the gradient of a scalar function, i.e. the velocity field can be described by a velocity potential. In the case of an incompressible flow the velocity potential satisfies Laplace's equation, for which there are many know solutions. This type of flow is typically referred to as Potential flow and there are many applications to real flows, e.g. Paterson (1983) pg 205-206.

Such that the motion of the fluid can be described by a scalar velocity Potential Φ, i.e.:

$$u = \nabla\Phi$$

The assumptions on which an ideal fluid is based are
1. Homogeneous and incompressible fluid ($\nabla . u = 0$)
2. Inviscid - viscosity can be neglected
3. Irrotational (i.e. $\nabla \times u = 0$)

Substituting this into the continuity equation Laplace's equation is derived.

$$\nabla^2\Phi = 0$$

Many solutions of Laplace's equation are known and can be used to represent certain aspects of real flows. Also, because Laplace's equation is linear the solutions can be added together to simulate a real flow which is created by a combination of effects.

The GH Blockage model adopts Potential flow theory and thus can utilise known solutions to Laplace's equation to simulate the flow field outside of a rotor streamtube. This method is a first approximation to the real flow and several key assumptions are made when using this approach. The next section reviews these assumptions.

4.2 Potential flow modelling assumptions

The assumptions of an ideal fluid are reviewed here to confirm that the use of Potential theory is appropriate for this application. Following this, a full description of the theory behind the GH Blockage Model is given.

The assumption that the fluid is incompressible is appropriate given the expected maximum changes of density. The density of water is a function of pressure, temperature and chemical consistency. Temperature changes from 0-20 degrees Celsius across the sea depth would equate to ≈ 1.6 kgm^{-3}, i.e. changes in density of less than 0.2%. The chemical consistency of the water has a greater effect, with sea water being ≈ 30kgm^{-3} denser than fresh water, but the change in chemical composition over a near scale will be negligible given the highly turbulent nature of the tidal resource. Thus the incompressible assumption is considered valid and allows for the use of the continuity equation.

The inviscid assumption is considered to be reasonable because the Reynolds numbers at the rotor scale for typical tidal flows are the order of 1e7 and thus viscous forces are assumed to be negligible when considering changes in the flow field.

The assumption that the flow is irrotational is an approximation, as there will be areas of concentrated vorticity generated by the high shearing of the fluid in the boundary layers over the turbine blades. The resulting vorticity is, however, generally contained within the bounding streamtube. As a first approximation it is assumed the wake rotation does not to affect the flow outside of the streamtube i.e. other than the flow in the streamtube and on the streamtube surface, the flow is irrotational (Thomson (2004) showed the amount of rotation in the wake to be less that 20% of the mean stream flow, supporting this assumption).

To predict the mean change in rotor operating state due to blockage effects no understanding of transient effects is required, thus the assumption that the flow is steady is valid.

The scalar velocity Potential term is derived through an understanding of the body forces applied to the flow. A review of possible body forces acting on the flow is provided to ensure the model captures the main physical processes:

1. Rotor momentum extraction: As the rotor extracts momentum a reaction force is imparted upon the flow in the form of a pressure field. This is the principal parameter to be accounted for by the model.

2. Gravitational Force: As the tide changes the depth of sea will change and although the bulk flow motion might be driven by a free surface pressure gradient, within the near scale at any instant in time the change in gravity head will be insignificant. Thus the mean affect of gravity is assumed to be constant on all parts of the flow.

3. Coriolis Force: The rotation of the Earth does affect the flow of oceans on the times scale of a day. But within the time scale of the rotor, i.e. 10-20 rotations per minute, the effect of changes in Coriolis force is negligible.

4. Acceleration Force: The free surface pressure gradient drives the tidal flow through two high tides per day. This time scale is far greater than the time it takes the flow to cross the near scale and thus the acceleration effect due to the changing tidal flow will be small and can be ignored.

In an attempt to quantify the impact of modelling assumptions on solution uncertainty, the following table summaries the impact of the main modelling assumptions. It should be noted that higher resolution models (i.e. models which incorporate more physical processes and are thus more complicated) may not provide a more accurate solution and can increase the solution uncertainty due to the added complexity.

Table 4.1 Impact of modelling assumptions

Assumption	Impact
Incompressible	This assumption is used by all the modelling methods, so there is no loss in model accuracy in comparison with other models. Power changes are directly proportional to density variations, thus the maximum uncertainty associated density variations is very small.
Inviscid	Viscous forces are of the order of 1/Re (1e-7). Thus the impact of not modelling them directly is assumed to be very small.
Irrotational	The exclusion of wake rotation (compared to using a vortex method) means that the flow will be less representative than the real flow conditions. Bounding surfaces will act to change rotor performance due to a change in the pressure field and as a result the wake rotation will alter. However, the model is used to evaluate relative changes in performance due to blockage (i.e. by comparing an irrotational boundless model with an irrotational bounded model).
No turbulence	Turbulent flow can be represented in a number of different ways (see Section.2.4.6). The exclusion of turbulence in the potential model means that there is no direct method to evaluate how any bounding surfaces may alter the fluctuating flow in such a way as to affect rotor performance. It is anticipated that bounding surfaces act to change the pressure field in the flow in such a way as to not affect the turbulence structure.

Mikkelsen (2003) compares tunnel blockage corrections for several different modelling methods and as can be shown in his results shown in Figure 4.1 below.

R_{tun}/R_{rot}	Eq.(6.15)	Eq.(6.14)	Actuator Disc
∞	1	1	1
10.0	1.004	1.004	-
3.33	1.045	1.032	1.034
2.5	1.072	1.052	1.053
2.0	1.112	1.073	1.075

Figure 4.1 Comparison of tunnel blockage corrections [Mikkelsen (2003)]

The second column (Eq. 6.15) is Glauert's well-know approximate solution to correct for tunnel blockage. The third column (Eq. 6.14) contains the results from 1-d the "corrected" actuator disc theory, which was outlined in Section 2.4.2. The fourth column (labelled "Actuator Disc") contains the results of the generalised actuator disc model developed by Mikkelsen, which is an axi-symmetric numerical solution to the Navier-Stokes equations in which the rotor is modelled as an actuator disc (i.e. a constantly loaded pressure surface). The "corrected" actuator disc theory gives very good agreement with the generalised actuator disc model i.e the numerical solution. Further work shows that even with a fully viscous CFD code, the discrepancies are small due to tip losses. This suggests that the simplified (corrected) actuator disc models demonstrate a high degree of accuracy when compared with more complicated methods. The move from a corrected actuator disc model to a Potential flow model is to incorporate 3-d effects such as asymmetric boundary proximity.

4.3 Potential flow model

The GH Blockage model uses Potential flow theory to simulate the steady flow field around a turbine's expanding streamtube. Standard solutions for the flow field generated from a point source in a uniform stream in an unbounded fluid can be combined with the principle of continuity to derive a model that is representative of a rotor operating in a uniform flow. The figure below provides a schematic of the Potential flow model. The red dot represents the source and the red shaded region represents the flow expelled from that source.

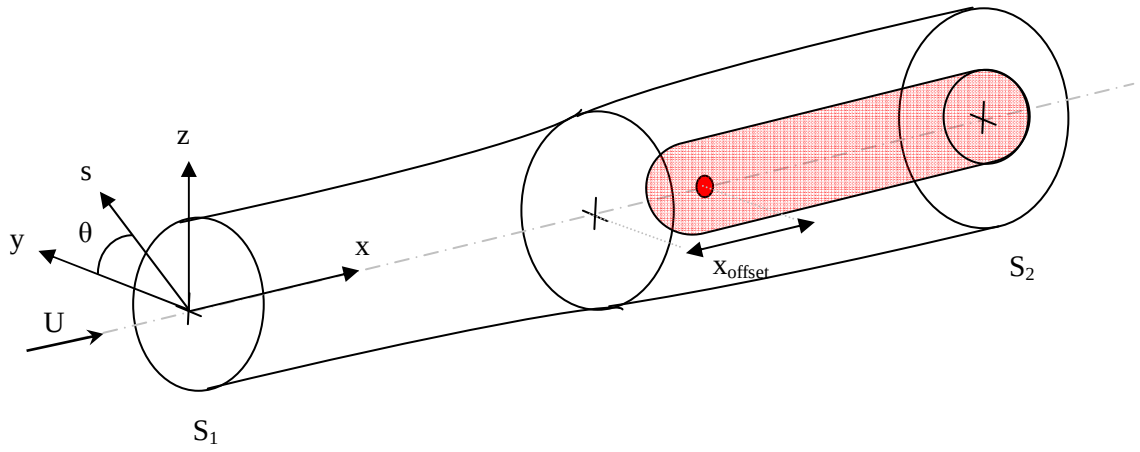

Figure 4.1 Schematic of the source and uniform flow model

In spherical coordinates the Potential flow model takes the form:

$$\phi = U_x - \frac{m}{4\pi r}$$

where U is the free stream velocity, m is the strength of the source and is equal to the volume flux expelled by the source, and r is the distance from the source. The velocity field is found by taking the grad of ϕ:

$$\nabla\Phi = \mathbf{u} = Ue_x + \frac{m}{4\pi}\frac{\mathbf{r}}{|\mathbf{r}|^3}$$

A rigorous three dimensional momentum integral over a control volume using this model has been conducted by Spalart (2003) and included in Appendix B for reference. This analysis yields the same result as classical 1-d actuator disc theory, hence verifying its suitability as a modelling method. The value of m can be evaluated in terms of the axial induction factor (a) or the thrust coefficient (Ct), using momentum analysis: Considering a control volume of a cylinder of cross-sectional area S_2 (as shown in Figure 4.1). The removal of energy from the flow causes it to expand, such that some of the volume flux leaves from the sides of the control volume. This means there is a difference in the volume flux across the ends of the control volume. To simulate the expansion of the wake the point source needs to inject this difference in volume flux, so that:

Mass flux from source (m) = Mass flux upstream – Mass flux downstream

Or

$$m = S_2U - S_2\alpha U$$

Using continuity S_2 can be described in terms of α, i.e.:

$$S_2 = S\frac{\alpha}{\beta} \qquad \text{where } \beta = \frac{1+\alpha}{2}$$

Thus,

$$m = \frac{1}{2} U \pi R^2 \frac{\left(1-\alpha^2\right)}{\alpha}$$

Or as a function of axial induction factor or Ct:

$$m = U \pi R^2 a\left(1-a\right) = U \pi R^2 \frac{Ct}{\left(1-Ct\right)^{0.5}} \qquad (4.1)$$

To leading order the source bends the streamlines as shown in Figure 4.1. There is a leading correction of order $1/r^3$ which corresponds to an offset in source location along the x-axis. The physical interpretation for this correction is the small amount of circulation induced on the surface of the streamtube. To evaluate this correction offset the model can be altered such that:

$$\mathbf{u} = \nabla \phi = U_{ex} + \frac{m}{4\pi} \cdot \frac{\mathbf{r} - \mathbf{r_s}}{\left|\mathbf{r} - \mathbf{r_s}\right|^3}$$

Where r_s is the offset vector from the origin, which is set at the turbine centre. To evaluate the rotor streamtube equation a volume flux balance is cylindrical coordinates can be used. Using:

$$s^2 = y^2 + z^2 \text{ and } r^2 = s^2 + x^2$$

In cylindrical coordinates the flux from source is:

$$q = \int_x^\infty \int_0^{2\pi} \frac{\partial \phi}{\partial s} s \cdot d\theta \cdot dx$$

$$q = \int_x^\infty 2\pi s \frac{\partial}{\partial s} \frac{m}{4\pi r} dx$$

$$q = \frac{m}{2} \int_x^\infty \frac{s^2}{\left(s^2 + x^2\right)^{3/2}} dx$$

which yields (as shown by Lighthill (1986)) to

$$q = \frac{m}{2}\left[1 - \frac{x}{r}\right]$$

Considering any area *a*, then the contribution of volume flux from the stream is *aU* and from the point source it is *q*. Incorporating the offset:

Flux in streamtube = Flux from uniform flow + Flux from source

$$= aU + \frac{m}{2} \cdot \left(1 - \frac{x - x_{offset}}{\left|\mathbf{r} - \mathbf{r_s}\right|}\right)$$

Selecting the rotor streamtube (i.e. that encompassing the rotor swept area at x=0) and conducting a volume flux balance across the end of the turbine streamtube, where the downstream crosssectional is S_2 and the the stream speed is U (the Potential model does not simulate the real flow inside the streamtube), the equation for the streamtube is:

$$S_2 U = U\pi R^2 + \frac{1}{2} m \left(1 - \frac{x_{offset}}{|\mathbf{r} - \mathbf{r_s}|} \right)$$

Solving for x_{offset}, using

$$S_2 = \pi R^2 \frac{2\alpha}{1+\alpha} \quad , \quad m = \frac{1}{2} U \pi R^2 \frac{\left(1-\alpha^2\right)}{\alpha} \quad \text{and} \quad \mathbf{r_s} = \begin{pmatrix} x_{offset} \\ 0 \\ 0 \end{pmatrix}$$

Yields:

$$\frac{2}{1+\alpha} = 1 - \frac{x_{offset}}{\sqrt{R^2 + {x_{offset}}^2}}$$

$${x_{offset}}^2 = \left(1 - \frac{2}{1+\alpha}\right)^2 \left(R^2 + {x_{offset}}^2\right)$$

$$\Rightarrow x_{offset} = \frac{(\alpha - 1)R}{2\sqrt{\alpha}} \qquad (4.2)$$

This approach is used within the GH Blockage model to incorporate additional 3-d effects. The method by which changes to performance are predicted is through the alteration in the streamtube shape. Note that this model only predicts the near field wake; it does not model the wake recovery process that happens after the pressure-driven wake expansion.

Additional turbines can be represented by the use of multiple sources. The introduction of the seabed as a rigid boundary can be easily introduced using the Method of Images. The Non-slip condition is not met, but a perturbation approach could be developed here. As a first approximation it is assumed that the non-uniform flow field can be normalised out. This will not be representative when there is significant seabed generated shear flow. However, this scenario will be avoided for most device installations due to the lower energy content in the bottom part of the boundary layer.

The generalised equation for multiple rotors and their image is:

$$\Phi_{Flow} = \Phi_{UniformStream} + \sum_{i=1}^{2} \Phi_{TurbineSource_i} + \sum_{j=1}^{2} \Phi_{\mathrm{Im}ageSource_j} \qquad (4.3)$$

The introduction of the free surface creates an additional boundary on top of the turbines which further bounds the flow. However, unlike the seabed the free surface has no 'no-slip' condition and is also able to move, such that the boundary can distort. This distortion can

appear in the form of surface waves which travel away from the surface disturbance. The boundary condition associated with a free surface disturbances in a uniform stream is known as the Neumann-Kelvin problem (discussed by Tuck and Scullen (2002)), and can be described by:

$$\frac{\partial \Phi}{\partial z} + K \frac{\partial^2 \Phi}{\partial^2 x} = 0$$

at the mean water level, where K is defined as:

$$K = \frac{U^2}{g}$$

Only when the Froude number reaches values greater than 0.1 will free surface effects become apparent; even then they are likely to be lost in the ambient waves. This problem has been studied in some detail for the application of wave resistance on submerged objects. Although Tuck and Scullen (2002) show the impact is small even at close proximity, it is expected that most device will operate away from the free surface to avoid wave loads. Experimental evidence to date has shown that when scaling to the Froude number, no visible surface depressions are observed (apart from support structure bow waves). Eyewitness reports of the flow down stream of MCT's SeaGen device also report no obvious surface disturbance generated when the rotors extract momentum. Thus the approximation of the free surface to a solid boundary is considered reasonable. For a confined channel the collective effect of momentum extraction may result in downstream head loss, but this effect is not considered as part of the near field blockage problem. Hence the initial assumption is that a solid body boundary can represent both the seabed and the free surface.

$$\frac{\partial \Phi}{\partial z} = w = 0$$

on z = 0, -h

However, using the "Method of Images" to model both boundary conditions above would require an infinite series of images sources, due to the interaction of the image sources on each other. The Multipole method, explained by Linton C.M. and McIver P (2001), is an alternative way to represent the solid boundary conditions at the seabed and the free surface. It can also be developed to incorporate the free surface wave effect, unlike the method of images. The Multipole method uses the solution of Laplace's equation for poles to find a separate linearly-independent solution which, based in a different coordinate system, satisfies the boundary condition. The Multipole method is adopted in the GH Blockage model.

Representing a single pole (i.e. a source with unit mass flux) using Bessel's equation in cylindrical polar coordinates yields the form:

$$\frac{1}{r} = \int_0^\infty e^{-\mu|z|} J_0(\mu s) d\mu$$

By solving for specific boundary conditions the Potential field around the outside of the bounding stream tube can then be described by:

$$\nabla\Phi = U + \frac{m}{4\pi}\begin{bmatrix} -\frac{x}{r^3} + \int_0^\infty \mu \frac{x}{s} e^{-\mu \cdot d} e^{\mu|z|} J_0^{'}(\mu s) d\mu \\ -\frac{y}{r^3} + \int_0^\infty \mu \frac{y}{s} e^{-\mu \cdot d} e^{\mu|z|} J_0^{'}(\mu s) d\mu \\ -\frac{z}{r^3} + \int_0^\infty \mu sign(z) e^{-\mu \cdot d} e^{\mu|z|} J_0(\mu s) d\mu \end{bmatrix} \quad (4.4)$$

A full derivation is provided in Appendix C.

The above equation is used to find the solution of the flow field for defined locations in the domain. However, the Multipole method is only valid at length scales equal to the distance from the bounding surfaces, therefore this method is generally restricted to the streamtube's near field. It is applicable for the purposes of performance characterisation, where the cross-sectional areas of the streamtube at 2-3 diameters from the rotor plane can be used to evaluate the changes in rotor performance.

As part of an iteration process to find the altered operating state, the one rotor parameter that is assumed to remain constant i.e. is independent of blockage, is the rotor resistance. Taylor (1944) defined the theoretical relationship between a resistance coefficient κ and the drag coefficient as:

$$C_T = \frac{\kappa}{\left(1 + \frac{1}{4}\kappa\right)^2}$$

Correlating this equation with the equation for Ct as a function of axial induction factor yields the rotor resistance coefficient as a function of Ct and axial induction factor:

$$\kappa = C_T (1-a)^2 \quad (4.5)$$

The rotor resistance coefficient is effectively the relationship between the flow onto the blades and the resulting force on the blades. It is assumed that this relationship is independent of blockage, which from a physical perspective appears reasonable. Thus it is assumed that a for a given change in axial induction factor, Ct will change to maintain a constant κ value.

In summary the key assumptions made are:

- Steady flow – for the analysis of performance change, the flow speed is constant.
- Inviscid – the high Reynolds numbers mean viscous forces will be small, and that changes to performance will not be affected by viscous effects.
- Irrotational – very little rotation is imparted into the flow by the wake streamtube. A correction for this is provided via linear momentum analysis.

- The pressure driven expansion of the streamtube can be represented by a simple source term and characterised by the boundless Ct.
- The non-slip condition is not modelled, as it is assumed that the mean flow over the rotor is uniform, leading to a uniform change in flow outside of the streamtube.
- The expected operational Froude numbers are low enough to ignore local surface disturbances.
- Rotor resistance coefficient is independent of blockage.

5 GH BLOCKAGE MODEL METHODOLOGY AND IMPLEMENTATION

This section describes how the GH Blockage model is incorporated into a working code for use in the GH TidalFarmer array modelling software tool.

The overall concept of the GH TidalFarmer modelling method is to reduce the extremely complex interactions between tidal turbines and the surrounding flow field in to a distinct physical process which can be simplified and modelled. Classical analysis simplifies the physical processes under investigation via the selection of an appropriate scale. The three appropriate scales of interest are Coastal basin, Array and Device scale (see Figure 5.1). The GH Blockage model is found at the "Device scale" level.

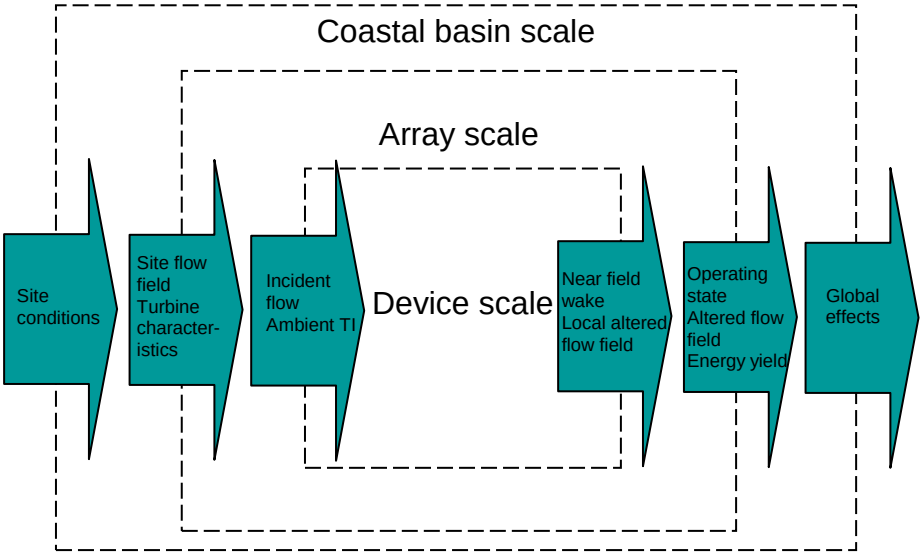

Figure 5.1: Hierarchy of modelling domains and scales

Within the "Device scale" level there are several mathematical models that are drawn upon. The figure below puts the GH Blockage model into context within the GH TidalFarmer software.

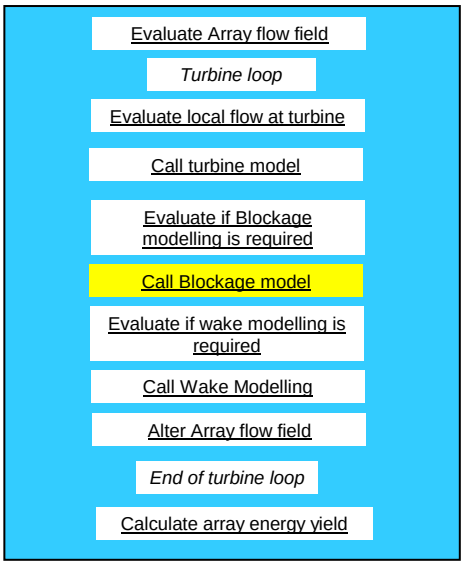

Figure 5.2: Overview of GH TidalFarmer software architecture showing the GH Blockage model in its context

As stated in Section 3 the GH Blockage model serves two purposes: To determine changes in turbine performance (Cp & Ct) and to alter the array flow field locally around the turbine under analysis. The sections below describe how both will be incorporated in to the GH TidalFarmer software.

5.1 Performance modelling

To predict the change in rotor performance and mean load (i.e. Cp and Ct) the GH Blockage model uses a set number of inputs. These are:

- The Boundless operating Cp and Ct (and TSR), evaluated via a lookup table given the local disc-averaged flow speed at the rotor location.
- The proximity of the sea-bed and free surface to the rotor
- The proximity of near field objects, such as adjacent turbines and channel walls
- The required accuracy for the calculation (i.e. set the grid size and modelling method) based on the iteration point in the optimisation loop.

Given these inputs a number of check routines are used to evaluate the model set-up. These include:

- Evaluate effective distances to boundaries and turbine groupings
- Evaluate the type of model to use (dependent on the required accuracy)
- An estimate of blockage correction from 2D theory to inform initial correction estimate in the Blockage model iteration

The main iteration loop is then initiated

- Set up the model, evaluate sources, strengths and offsets.
- For each turbine in the group in turn:
  - Calculate the flow field on and around the expected streamtube shape. Only the flow outside of the bounding streamtube is representative of the real flow and thus the first part of the analysis is to evaluate this streamtube.
  - Use streamlines which flow past the edge of the rotor disc to calculate the altered streamtube shape.

  - Evaluate the change in streamtube shape i.e. the upstream and downstream cross-sectional areas
- Evaluate the error in rotor resistance for each turbine in the group.
- Propose new rotor operating states for each turbine in the group
- Iterate until the errors are within tolerance
- Evaluate altered Cp, Ct and TSR

The flow diagram below illustrates the performance modelling approach to find the altered rotor Cp and Ct:

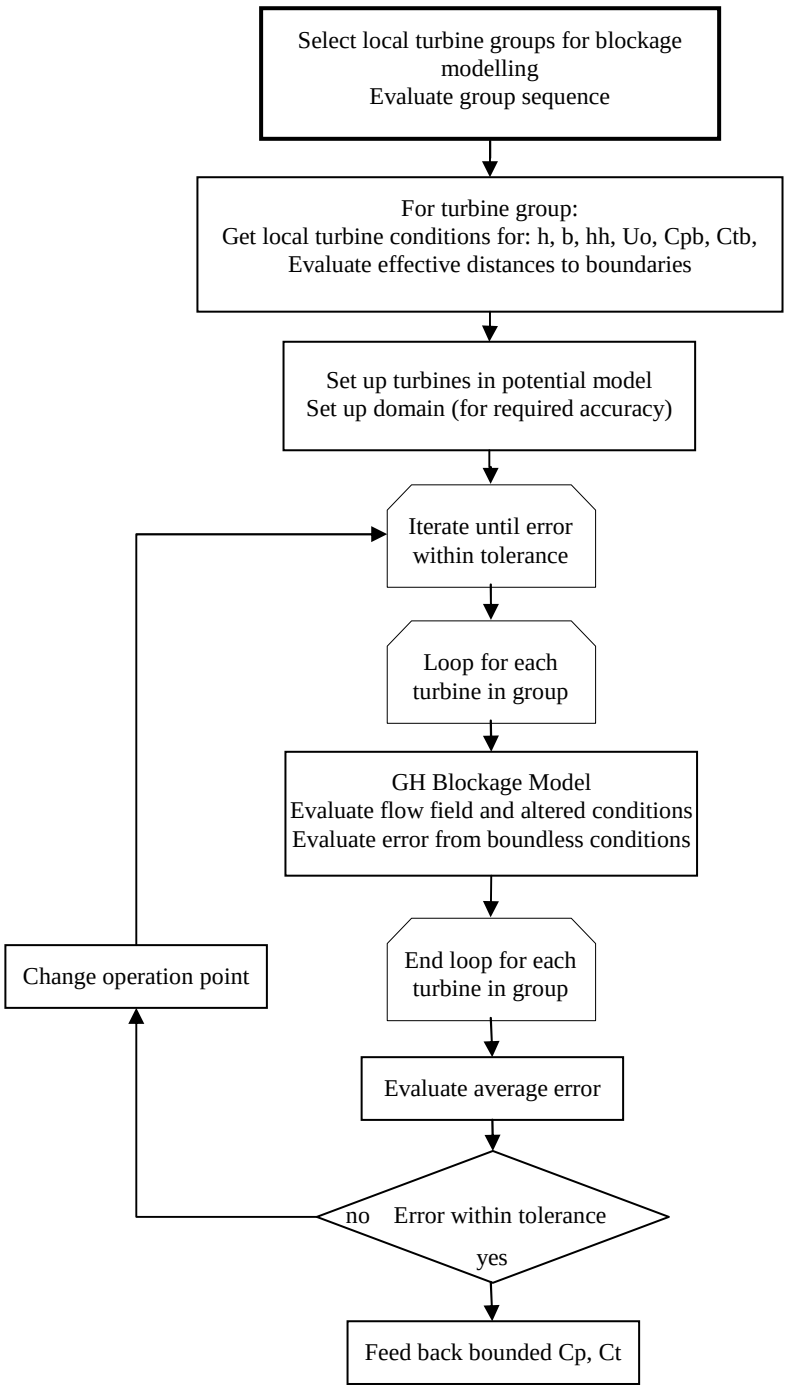

Figure 5.3 Flow diagram of the GH Blockage model: Performance modelling

An example of the effect of local blockage in 3-d is provided below to demonstrate the possible changes in performance and thrust as a result of bounding effects.

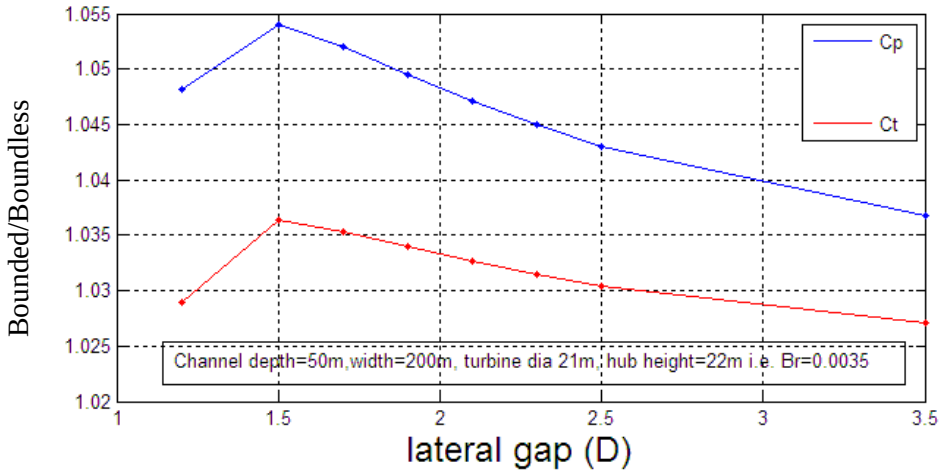

Figure 5.4 Example of blockage effect using GH Blockage model

5.2 Flow field modelling

Once the change in performance due to blockage has been calculated, the altered Cps and Cts are used to evaluate the local flow field outside of the streamtube. The flow field modelling uses the GH Blockage model to predict the local flow field around the rotors of interest.

Inputs:

- Altered Cps and Cts for the group of turbines of interest
- The proximity of the sea-bed and free surface to the rotor
- The proximity of near field objects, such as adjacent turbines and channel walls

The main procedure is as follows:

- Evaluate effective distances to boundaries and turbine groupings
- Set up the model, evaluate sources, strengths and offsets.

For the group of turbines calculate the flow field on and around the rotor streamtubes (typically up to 3D around the rotor).

- Alter the array flow field using a perturbation approach

The following flow diagram outlines the above process:

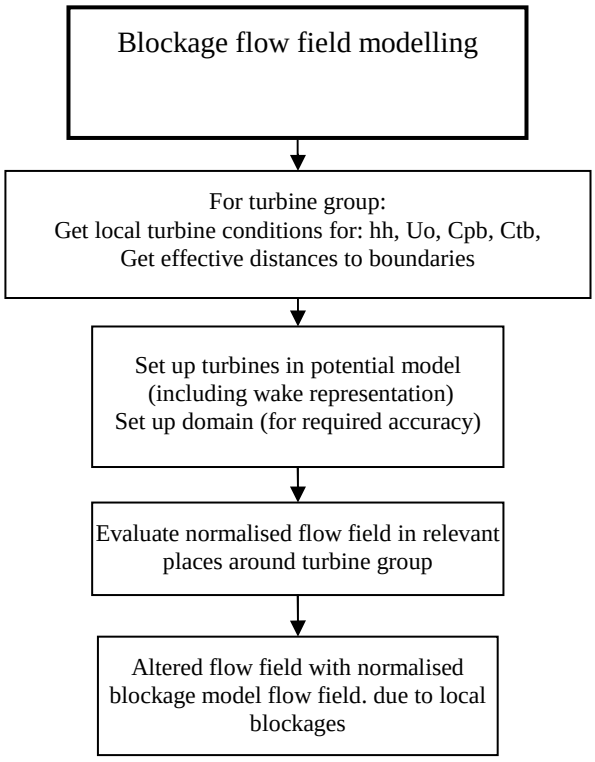

Figure 5.5 Flow diagram of the GH Blockage model: Flow Field modelling

The figure below visualises an example of how the flow changes around two turbines placed 2.5D apart.

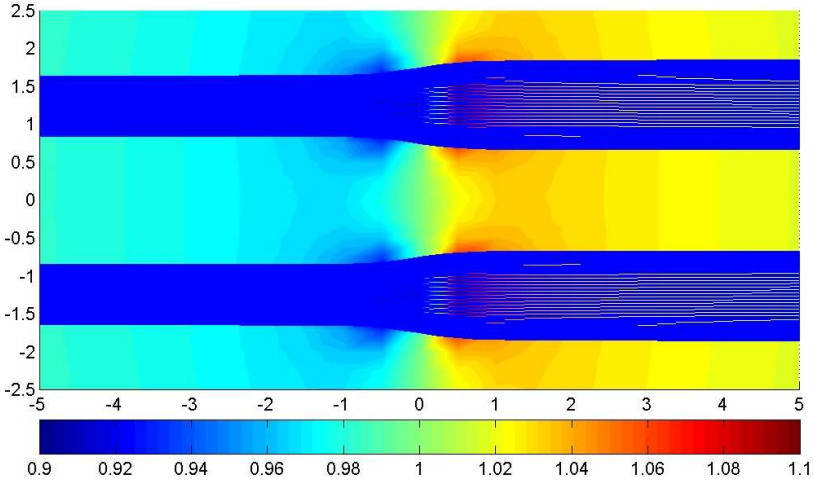

Figure 5.6. Blockage model of two turbine streamtubes (blue lines) - cut through the centre of the flow field

5.3 Implementation

The GH TidalFarmer software tool will consist of a single executable file (user interface) with which the user will interact, as well as a number of calculation modules which will be implemented as dynamic-link libraries (DLLs). Tidal calculations will be controlled and coordinated by a top-level "core functionality" module. The GH Blockage model is likely to

be implemented as a subsidiary module (DLL) providing a service to the top-level DLL via a clearly-specified interface. This means that, as far as the top-level DLL is concerned, the GH Blockage DLL and others are "black boxes" whose internal functionality does not need to be known. This is in accordance with the principles of good software design.

Choosing the most appropriate programming language depends on the method of investigation and how the results will be analysed. Currently the code is written as a Matlab script, which allows for easy interrogation and analysis.

The user interface is likely to be written in a .NET language such as C#, while the modules which do the actual calculations will either remain in Matlab or migrate to another language, such as Fortran or C++. The top-level DLL will call the Blockage DLL at the appropriate point in the speed, direction and optimisation loop. Typically blockage modelling will be conducted towards the end of an optimisation iteration and when lateral spacings are being investigated.

Both the altered Ct and surrounding flow field will be fed into the wake modelling module. The altered Cp is stored and used at the end of the entire calculation to predict annual energy yield.

Table 5.1 Summary functional description

Model	Inputs	Outputs	Method used
Blockage model	Incident 3-d flow field Boundless turbine characteristics (Cp_b, Ct_b) Turbine locations	Altered turbine performance characteristics (Cp, Ct)	Blockage performance model
		Altered 3-d flow field around turbine.	Blockage flow field model

Table 5.2 Detailed functional description of the Blockage performance model

Task	Input	Output	Method
Select local turbine groups for blockage modelling Evaluate group sequence	Turbine locations, Flow direction, Criteria for proximity (radial distance apart)	Selected turbine group (turbine locations)	Proximity algorithm.
For turbine group: Get local turbine conditions Evaluate effective distances to boundaries	Selected turbine group (turbine locations)	For each selected turbine: Turbine locations Local geography: Water depth, distance to channel walls, hub height. Operating condition: Uo, Cpb, Ctb.	Lookup algorithm
Set up turbines in potential model	For each selected turbine: Turbine locations Local geography: Water depth, distance to channel walls, hub height. Operating condition: Uo, Cpb, Ctb.	Model set-up	Using equations 4.1 to 4.3 to set model parameters.
Set up domain (for required accuracy)	Point in optimisation loop. Predefined settings.	Domain on which to solve the model defined	Matrix set-up algorithm
Loop for each turbine in group			
Evaluate flow field and altered conditions	Model set-up	Flow field solution Calculated change in rotor performance	Solve equation 4.4 on model domain Use equation 4.5 to establish new rotor resistance
Evaluate error from boundless conditions	Model set-up (no boundaries included) Operating condition: Uo, Cpb, Ctb.	Model Error	Solve simplified equation 4.4. Actuator disc theory
End loop for each turbine in group			
Evaluate average error			
Iterate until error within tolerance	Collective resistance error	Iteration requirement	Comparison algorithm
Change operation point	Individual resistance error	Altered model inputs for next iteration.	Iteration algorithm
Feed back bounded Cp, Ct		Altered rotor performance	

Table 5.3 Detailed functional description of the Blockage flow field model

Task	Input	Output	Method
For turbine group: Get local turbine conditions Evaluate effective distances to boundaries	Selected turbine group (turbine locations)	For each selected turbine: Turbine locations Local geography: Water depth, distance to channel walls, hub height. Operating condition: Uo, Cpb, Ctb.	Lookup algorithm
Set up turbines in potential model (including wake representation)	For each selected turbine: Turbine locations Local geography: Water depth, distance to channel walls, hub height. Operating condition: Uo, Cp, Ct (i.e. blockage corrected values).	Model set-up	Using equations 4.1 to 4.3 to set model parameters.
Set up domain (for required accuracy)	Predefined settings.	Domain on which to solve the model defined	Matrix set-up algorithm
Evaluate normalised flow field in relevant places around turbine group	Model domain Model set-up	Flow field solution	Solve equation 4.4 on model domain
Alter flow field with normalised blockage model flow field due to local blockages	Blockage induced flow field	Combined flow field	Flow field combination algorithm

6 VALIDATION

6.1 Existing verification

The blockage correction theory outlined in Section 2.4.3 has been used to partly verify the potential model proposed by GH. A 3-d version of the potential model has been compared to the 3-d symmetric actuator disc tunnel model and an equivalent 2-d actuator disc channel model (where the equivalent rotor area is changed to maintain the same Blockage ratio). The figure below shows a small change in correction when comparing the tunnel and channel theory. This is mainly due to the very low Froude Numbers expected in tidal stream. The GH model compares well with the actuator models. The correlation deteriorates at higher blockage ratios, but realistic blockage ratios are not likely to exceed 30%. In this region the model performs well.

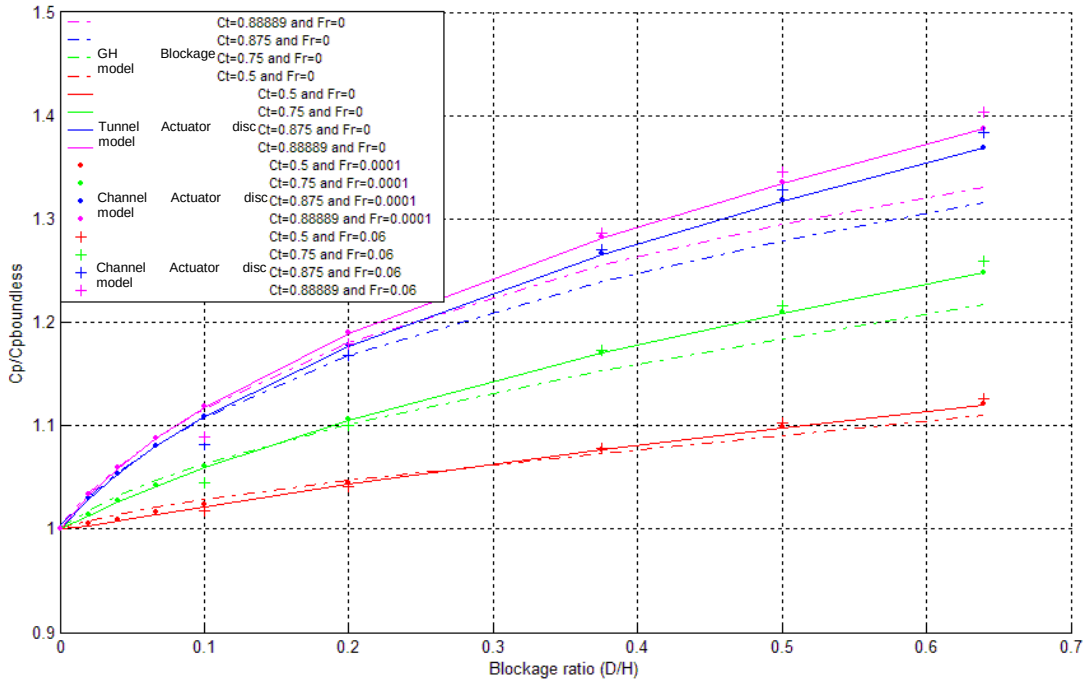

Figure 6.1 Comparison of 2D blockage potential model results and theoretical solutions

Whelan [2009] demonstrated the suitability of using 1-d corrected actuator disc theory for a highly blocked rotor. But to date a full experimental investigation of the impact of proximity of bounding surfaces on rotor loads and performance has not been conducted. It is thus the intention of the PerAWAT project to provide suitable validation data. Details of this are covered in the following section.

6.2 Developments under PerAWAT

There are several investigations into the effects of bounding surfaces within the PerAWAT project. At the device scale the effect of the free-surface will be characterised through both experimental and numerical investigations. Numerical modelling in WG3WP1 will investigate the effect free-surface proximity on an HA axial flow rotor. This will be cross compared with WG3WP5. Similar analysis for both a ducted and open centre rotor will be analysed in WG3WP1 and WG3WP5 respectively. In WG4WP1 the effect of blockage and interaction with the free-surface will be investigated with two tests in which the water depth is altered. WG4WP3 will conduct similar tests for both ducted and open-centre devices. The prime area for investigation in WG4WP2 is in the impact of varying the lateral spacing

between rotors. In addition one test will investigate the impact of depth variation. In WG3WP2 numerical modelling will be conducted for two scenarios: an isolated depth constrained rotor; and an infinitely wide depth constrained array. This will yield one test case to which comparisons can be made.

Rotor performance and loading data from the ReDAPT (Reliable Data Acquisition Platform for Tidal) project will also be utilised if available. This data will further validate the application of this model for full scale scenarios.

The wide variety of numerical and physical validation tests will provide a robust set of tests to which the GH Blockage model can be compared. The GH Blockage model will be set up to be directly analogous with each test allowing direct comparison and thus validation of the model. The input parameters for comparison will be; the proximity to boundaries and the measured/calculated boundless prediction of rotor performance. The output parameters for comparison will be the altered rotor thrust coefficient and, if feasible, the rotor power coefficient. Mapping the flow in the regions around the wake (as planned in WG4WP2) will also provide further evidence of the more complex interactions between adjacent rotors.

As shown in Section 6.1 above there appears to be a limit to the validity of this model and it is the intension to fully investigate the region of model applicability and the uncertainty associated with the modelling method. This will be done through the comparison with the test data (which itself has associated uncertainties) and through an understanding of order of magnitude of the error each modelling assumption introduces.

The applicability of this method to the ducted and open centre rotor type will also be investigated. Developments to the model may include general theories (Jamieson, 2008) developed for ducted rotors.

As with any numerical modelling approach there is a trade off between accuracy and computational time. At present the run times would be prohibitive to be included within an array design optimisation routine, but can be used at the final design iteration stage. The impact of calculation resolution will be investigated to assess the impact that model accuracy has on computational time and model uncertainty.

7 BIBLIOGRAPHY

Antheaume, S., Maıtre, T., Achard, J-L, (2008). *Hydraulic Darrieus turbines efficiency for free fluid flow conditions versus power farms conditions*, Renewable Energy 33, 2186–2198.

Bai, K. J. (1979). *Bloackage correction with a free surface.* J. Fluid Mech. 94 (3). 433-452

Bai, L., Spence, R. R. G., Dudziak, G. (2009). *Investigation of the Influence of Array Arrangement and Spacing on Tidal Energy Converter (TEC) Performance using a 3-Dimensional CFD Model*. EWTEC 2009

Betz, A. (1920). *Das Maximum der theoretisch möglichen Ausnützung des Windes durch Windmotoren*. Zeitschrift für das gesamte Turbinenwesen 26, 307-309.

Blunden L. S. et al. (2009). *Comparison of boundary-layer and field models for simulation of flow through multiple-row tidal fences*. Proceedings Eighth European Wave and Tidal Energy Conference, Uppsala, Sweden, pp 576-585

Bossanyi, E. A. (2007). *GH Bladed - Theory Manual, Technical Report.* 282/BR/009, Garrad Hassan and Partners Ltd.

Breslin, J. P., Andersen, P. (2003). *Hydrodynamics of ship propellers*. Cambridge Ocean Technology Series 3. Cambridge University Press

Burton, T., Sharpe, D., Jenkins, N., Bossanyi, E. (2001). *Wind energy handbook*. John Wiley and Sons.

Durgun, O., Kafalii, K. (1991). *Blockage Correction*. Ocean Engng, Vol. 18, No 4, pp. 269-282

Ewald, B. F. R. (ed.) (1998). *Wind tunnel wall corrections [La correction des effets de paroi en soufflerie]*. Advisory Group for Aerospace Research and Development (AGARD), Report No. AGARD-AG-336

Fraenkel, P. L. (2006). *Marine current turbines: pioneering the development of marine kinetic energy converters*. Proc. IMechE Part A: J. Power and Energy, 221, 159-169.

Gant, S., Stallard, T. (2008). *Modelling a tidal turbine in unsteady flow*. Proceedings of the Eighteenth (2008) International Offshore and Polar Engineering Conference, Vancouver, BC, Canada. 473-479

Garrett, C., Cummins, P. (2007). *The efficiency of a turbine in a tidal channel*. Journal of Fluid Mechanics, 588, 243–251

Glauert, H. (1933). *Wind tunnel interference on wings, bodies and airscrews*. Aeronautical Research Committee, Reports and Memoranda no. 1566

Gretton, G. I., Bruce, T., Ingram, D. M. (2006). *Hydrodynamic modelling of a vertical axis tidal current turbine using CFD*, Proceedings of the 9th World Renewable Energy Congress, Florence, Italy

Harrison, M. E., Batten, W. M. J., Myers, L. E., Bahaj, A. S. (2009). *A comparison between CFD simulations and experiments for predicting the far wake of horizontal axis tidal turbines*. Proceedings Eighth European Wave and Tidal Energy Conference, Uppsala, Sweden, 7-10 September 2009, pp 566-575

Jamieson, P. (2008). *Generalized Limits for Energy Extraction in a Linear Constant Velocity Flow Field*. Wind Energy 11 (5), 445-457

Laino, D. J. (2005). *NWTC Design Codes (AeroDyn).* [Online] Available at: http://wind.nrel.gov/designcodes/simulators/aerodyn/

Li, Y., Calisal, S. M. (2007). *Preliminary results of a vortex method for stand-alone vertical axis marine current turbine*. Proceedings of the International Conference on Offshore Mechanics and Arctic Engineering (OMAE2007-29708)

Lighthill, J. (1986). *An informal introduction to theoretical fluid mechanics*. Clarendon Press

Maskell, E. C. (1963). *A theory of the blockage effects on bluff bodies and stalled wings in a closed wind tunnel*. Aeronautical Research Council, R. & M., No. 3400

Massey, B. S. (1989). *Mechanics of fluids*. Chapman & Hall. Sixth Edition

Mikkelsen, R. (2003). *Actuator Disc Methods Applied to Wind Turbines*. PhD Thesis, Department of Mechanical Engineering, Technical University of Denmark

Newman, J. N. (1977). *Marine hydrodynamics*. The MIT Press

Paterson, A. R. (1983). *A first course in fluid dynamics*. Cambridge University Press

Prandtl, L., Tietjens, O. G. (1957). *Fundamentals of Hydro- and Aeromechanics*. Dover Publications. Re-print of 1934 edition

Rae, W. H., Pope, A. (1984). *Low-Speed Wind Tunnel Testing*. Wiley-Interscience

Scott, J. R. (1976). *Blockage correction at sub-critical speeds.* Transactions of the Royal Institution of Naval Architects 118, pp. 169–179

Snel, H. (2003). *Review of Aerodynamics forWind Turbines*. Wind Energy 6, 203-211

Spalart, P. R. (2003). *On the simple actuator disk*. Journal of Fluid Mechanics 494, 399-405

Strickland, J., Webster, B., & Nguyen, T. (1979). *Vortex model of the Darrieus turbine - analytical and experimental-study*. J Fluids Eng 101 101 (4), 500-505.

Tangler, J. L. (2002). *The nebulous art of using wind tunnel airfoil data for predicting rotor performance.* Wind Energy 5 (2-3), 245-257

Taylor, G. I. (1944). *Air resistance of a at plate of very porous material*. ARC Reports and Memoranda (2236)

Tuck, E.O., Scullen, D.C. (2002). *A comparison of linear and nonlineaer computations of waves made by slender submerged bodies*. Journal of Engineering Mathematics 42 (2002), 255-264.

O'Doherty, D. M., Mason-Jones, A., O'Doherty, T., Byrne, C. B., (2009). *Experimental and Computational Analysis of a Model Horizontal Axis Tidal Turbine*. Proceedings of the 8th European Wave and Tidal Energy Conference

Thomson, M. D. (2004). *The flow around marine current turbines*. MSc Thesis, Faculty of Science, University of Bristol

Topper, M., in progress. *Application of a Potential Flow Model to the Hydrodynamic Interaction between a Tidal Turbine, its Wake and the Free-Surface*. PhD University of Edinburgh.

van Bussel, G. J. W. (1999). *An assessment of the performance of diffuser augmented wind turbines (DAWT's).* Proceedings of the 3rd ASME/JSME Joint Fluids Engineering Conference, San Francisco, USA

Wang, T., Coton, F. N. (2000). *Prediction of the unsteady aerodynamic characteristics of horizontal axis wind turbines including three-dimensional effects*. Proc Instn Mech Engrs Vol 214 Part A, 385-400

Whelan, J. I. (2009). *A fluid dynamic study of free-surface proximity and inertia effects on tidal turbines.* PhD Thesis, Department of Aeronautics, Imperial College London.

Wilson, R. E., Lissaman, P. B. S. (1974). *Applied aerodynamics of wind power machines*. NTIS PB 238594, Oregon State University

Zahle, F. et al. (2007). *Wind turbine rotor-tower interaction using an incompressible overset grid method*. AIAA 45th Aerospace Sciences Meeting and Exhibit, Reno, Nevada

APPENDIX A - SPECIFIC ENERGY AND THE FROUDE NUMBER

When a rotor is bounded within an open channel, the flow is bounded by three rigid boundaries and one free surface. The free surface is dynamic and capable of depth variations, thus the governing forces of the flow must include gravity. Bernoulli's equation can still be applied to a flow with a one-dimensional height variation and hence a similar analysis to the boundless condition can be applied. However, the effect of removing momentum from an open channel, with a constant inflow, can affect both upstream and downstream conditions. The specific energy and dimensionless Froude number of a flow are used to investigate the relationship between the upstream and downstream flow conditions.

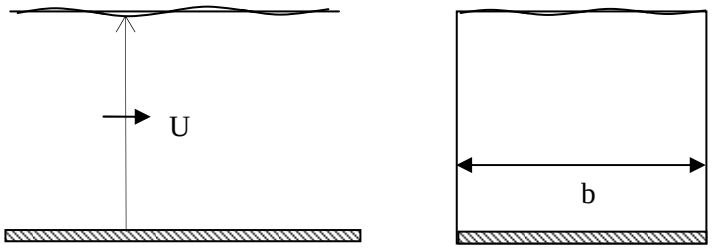

Figure A.1. Uniform flow in an open channel

The specific energy for a one dimensional channel flow, relative to the channel floor, is:

$$E = Z + w.U^2/(2.g) = Z + w.q^2/(2.g.A^2) \qquad (A.1)$$

where A = Z.b, where b is the channel width and q is the channel flow rate. w is the kinetic energy correction factor and accounts for a real flow not being completely uniform. Thus the true kinetic energy at a cross section is not necessarily equal to the spatially-averaged energy. For the uniform channel w = 1.

Assuming the inflow is constant and that the channel geometry does not vary, then

$$E = Z + q^2/(2.g.(Z.b)^2) \qquad (A.2)$$

Or

$$Z^3 - E.Z^2 + q^2/(2.g.b^2) = 0 \qquad (A.3)$$

This cubic yields two real positive solutions for Z, given any real values of E, q, g and b. The minimum specific energy point if found by differentiating the energy equation to find a depth at which the flow changes characteristics. This depth is known as the critical depth (Zc);

$$Zc = (q^2/(g.b^2))^{1/3} \qquad (A.4)$$

When Z=Zc

$$Zc.g = U^2 \qquad (A.6)$$

At this critical depth the inertia force balances the gravitational force. The Froude Number is the dimensionless number used to describe the ratio between these two forces in a given flow:

$$Fr = \frac{\text{inertia force}}{\text{gravity force}} = \frac{U}{\sqrt{(g.Z)}} \qquad (A.7)$$

If the incoming flow has Fr < 1 (or Z > Zc) then the flow is governed by gravitational forces and is described as subcritical or tranquil. In this type of flow the weight of the fluid

upstream drives the flow downstream and hence the downstream conditions affect the upstream conditions. To investigate how the removal of energy affects the depth downstream the specific energy of the flow is evaluated.

The figure A.2 below plots the change in specific energy of a flow with depth (relative to the critical depth) using a specified channel geometry and flow rate. The flow characteristics are governed by a single specific energy curve because the flow rate is fixed. It can be seen in the plot that a drop in energy from a tranquil flow can only result in a drop in depth and a resulting increase in speed (ΔU is relative to the uniform incoming flow speed). The red lines demonstrate that removing ~10% of specific energy affects the flow differently depending on the depth. If the depth is closer to the critical depth the result of energy extraction is a greater change in speed rather than depth.

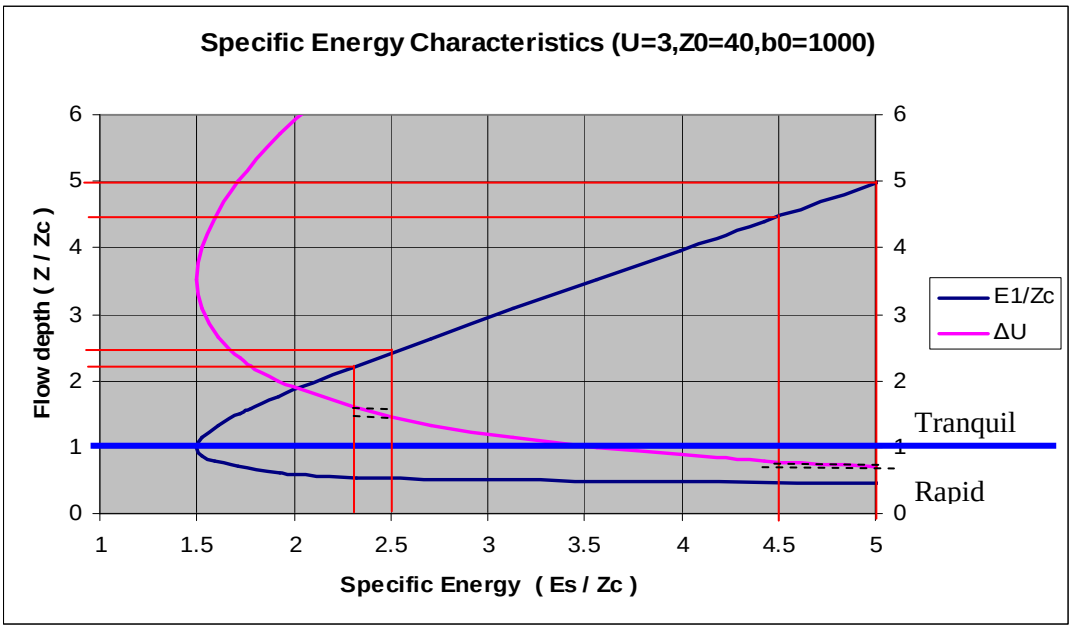

Figure A.2 Graph of channel flow specific energy

The change in Z/Zc due to the removal of a set amount of energy results in a depth and velocity change. The graph below demonstrates that for a varying depth channel the change in Z/Zc is the same as that for a shallower channel.

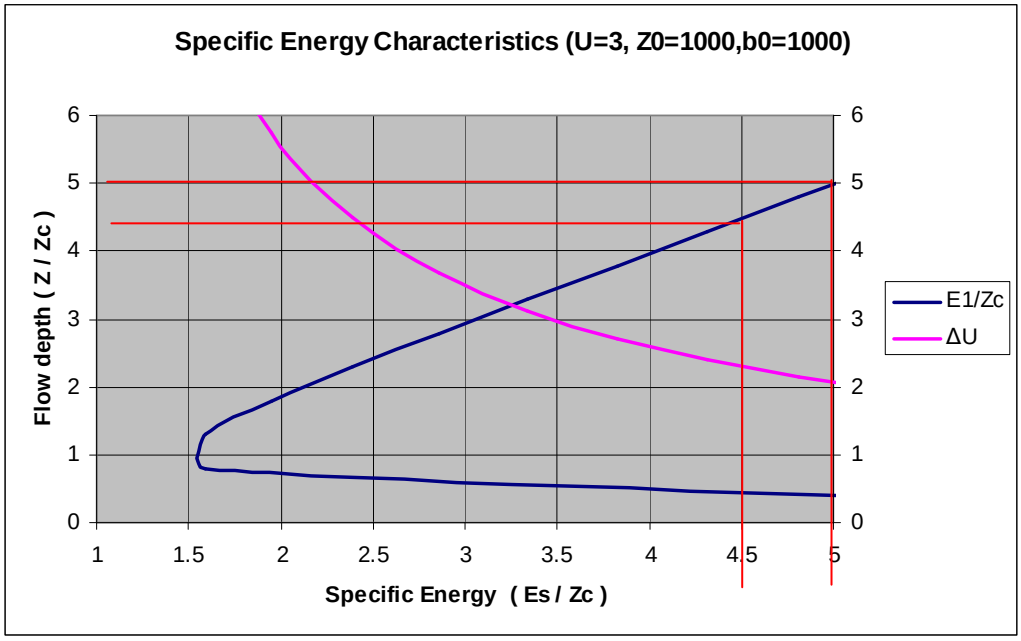

Figure A.3 Graph of deep channel flow specific energy

However, the value of Z/Zc is not constant with depth. By assuming that the critical depth does not vary significantly during energy extraction, the following relationship can be used to investigate the drop in height (ΔZ) as depth increases:

$$\Delta Zs^3/Zs = \Delta Zd^3/Zd \qquad \text{(A.8)}$$

where s and d denote a shallow and deep depth respectively. Thus as the channel depth increases the change in depth, due energy extraction, becomes much smaller and it tends towards the boundless condition.

Thus given the channel geometry, an inflow rate and the amount of energy extraction (or momentum removed), the resulting depth change can be found. To evaluate how much energy/momentum can be extracted from a free surface flow, a momentum balance must applied.

APPENDIX B – VALIDATION OF ACTUATOR DISC THEORY USING A POTENTIAL FLOW MODEL

This work has be done by Spalart(2003) but is repeated here. The momentum integral is taken over a control volume for which the far velocity field is predicted by the potential model. Note the main benefit of this analysis is that no assumption that velocity through the disc is aligned to the x axis is uniform is needed.

Conducting a momentum balance access control volume of a sphere $r >> R$

$$\int_0^{\pi}\int_{arcsin(R_2/r)}^{\pi} M_{\text{in}} d\theta d\phi = M_{\text{taken out}} + \int_0^{\pi}\int_0^{arcsin(R_2/r)} M_{\text{out thro wake}} d\theta d\phi \tag{A.1}$$

where M_{in} is the x-direction momentum entering the sphere, $M_{\text{taken out}}$ is the momentum taken out by the actuator disc (represented by a jump in pressure across the disc) and $M_{\text{out thro wake}}$ is the momentum leaving the sphere through the wake at a velocity of αU.

$$\begin{aligned} M_{\text{in}} &= -(u_x \mathbf{u}\cdot\mathbf{e}_r + p\mathbf{e}_x\cdot\mathbf{e}_r) \\ M_{\text{taken out}} &= \pi R^2 \Delta p \\ M_{\text{out thro wake}} &= \rho\pi R_2^2(\alpha U)(\alpha U) \end{aligned}$$

with axisymmetric flow and taking the integral from $\theta = 0$ in the +ive x direction to π in the -ve x direction, then

$$-2\pi r^2\rho\int_{arcsin(R_2/r)}^{\pi} u_x\mathbf{u}\cdot\mathbf{e}_r\sin\theta d\theta - 2\pi r^2\int_0^{\pi} p\mathbf{e}_x\cdot\mathbf{e}_r\sin\theta d\theta = \pi R^2\Delta p + \rho\pi R_2^2(\alpha U)^2 \tag{A.2}$$

To find the pressure field we can apply Bernoulli's equation to any streamline upstream of the actuator disc. A pressure jump (Δp) is added to the fluid that goes through the wake, but it is assumed that the pressure in the fluid that went through the actuator disc dissipatedsto p_{inf} at the control volume boundary, and thus the wpressure field can be found by

$$\text{outside the wake } p_\infty + \frac{\rho}{2}U^2 = p + \frac{\rho}{2}|\mathbf{u}|^2 \tag{A.3}$$

$$p = p_\infty + \frac{\rho}{2}U^2 - \frac{\rho}{2}\left(U^2 + 2U\frac{m}{4\pi}\frac{x}{r^3} + O\left(\frac{1}{r^3}\right)\right) \tag{A.4}$$

$$\tag{A.5}$$

Substuting the above in to the momentum equation

$$\begin{aligned} -2\pi r^2\left(\rho\int_{arcsin(R_2/r)}^{\pi} u_x u_r\sin\theta d\theta + \int_0^{\pi} p_\infty + \frac{\rho}{2}U^2 - \frac{\rho}{2}\left(U^2 + 2U\frac{m}{4\pi}\frac{\cos\theta}{r^2}\right)\cos\theta\sin\theta d\theta\right) \\ = \pi R^2\Delta p + \rho\pi R_2^2(\alpha U)^2 \end{aligned} \tag{A.6}$$

Substitute eqaution

$$-2\pi r^2\rho\int_{arcsin(R_2/r)}^{\pi}\left(U+\frac{m}{4r^2}\cos\theta\right)\left(U\cos(\theta)+\frac{m}{4r^2}\right)\sin\theta d\theta$$

$$-2\pi r^2\int_0^{\pi}p_\infty+\frac{\rho}{2}U^2-\frac{\rho}{2}\left(U^2+2U\frac{m}{4\pi}\frac{\cos\theta}{r^2}\right)\cos\theta\sin\theta d\theta=\pi R^2\Delta p\quad+\rho\pi R_2^2(\alpha U)^2+O\left(\tfrac{1}{r}\right)\qquad(A.7)$$

The above integral gives

$$R^2\Delta p=\rho R_2^2U^2(\alpha^2-\alpha)\qquad(A.8)$$

using Bernolli on a streamline in the wake

$$\text{inside the wake } p_{disc}+\Delta p+\frac{\rho}{2}(U_{disc})^2=p_\infty+\frac{\rho}{2}(\alpha U)^2$$

equating p_{disc} either side of the disc

$$p_\infty+\frac{\rho}{2}U^2=p_{disc}+\frac{\rho}{2}\left|\mathbf{u}_{disc}\right|^2$$

Thus the relationship between Δp and α is found for a given U as

$$\Delta p=\frac{\rho}{2}U^2(\alpha^2-1)\qquad(A.9)$$

Hence we see that the classical results are obtained which provide confidence in the use of Actuator disc theory.

APPENDIX C – MULTIPOLE METHOD

The potential for a single pole (a source of unit mass flux) in spherical polar coordinates is

$$\chi = \frac{1}{r}, \qquad \text{and } r = R\sqrt{(x^2 + y^2 + z^2)}$$

Bessel's equation is

$$\left(\frac{\partial^2}{\partial x^2} + \frac{\partial^2}{\partial y^2}\right)\left(e^{\pm\mu z} J_0(\mu s)\right) = -\frac{\partial^2}{\partial z^2}\left(e^{\pm\mu z} J_0(\mu s)\right) = -\mu^2\left(e^{\pm\mu z} J_0(\mu s)\right)$$

where $s = \sqrt{(x^2 + y^2)}$ and J_0 is the Bessel function of the first kind. Using Bessel's equation the equation (4.8) for a source can to be converted into a cylindrical polar coordinate system, by representing the pole as an integral, of the form

$$\frac{1}{r} = \int_0^\infty e^{-\mu|z|} J_0(\mu s) d\mu$$

The Multipole method uses a linearly independent solution to the above integral to fit the boundary conditions. Thus the total potential of χ becomes the summation of the pole solution and the linearly independent solution

$$\chi(\mathbf{r}) = \frac{1}{r} + \int_0^\infty A(\mu) e^{+\ \mu|z|)} J_0(\mu s) d\mu$$

The value of the constant A is found by applying boundary conditions at either surface. Checking the above solution still behaves as a source when $r \to 0$, it is seen that as $r \to 0$, $z \to 0$ and thus $\chi \to 1/r$, which is the solution for a source. However, as $r \to \infty$ the solutions will not be similar and the point at which they diverge will be governed by $A(\mu)$. To find $A(\mu)$ the boundary condition at the free surface is applied

$$\frac{\partial \chi}{\partial z} = 0, \qquad \text{on } z = \frac{d}{2}$$

Equation above is solved to find $A(\mu)$

$$\begin{aligned} \frac{\partial \chi}{\partial z} = 0 &= \int_0^\infty \left(-\mu e^{-\mu d/2} + \mu A(\mu) e^{\mu d/2}\right) J_0(\mu s) d\mu \\ \to A(\mu) &= e^{-\mu d} \end{aligned}$$

and similarly on the seabed

$$\frac{\partial \chi}{\partial z} = 0, \qquad \text{on } z = -\frac{d}{2}$$

and it is seen that the solutions agree

$$\begin{aligned} 0 &= \int_0^\infty \left(+\mu e^{-\mu d/2} - \mu A(\mu) e^{\mu d/2}\right) J_0(\mu s) d\mu \\ A(\mu) &= e^{-\mu d} \end{aligned}$$

Substituting in this value of $A(\mu)$ the potential χ becomes

$$\chi = \frac{1}{r} + \int_0^\infty e^{-\mu d} e^{\mu|z|} J_0(\mu s) d\mu$$

Applying this potential to the model, the total potential for a source at the origin in a uniform stream bounded by two solid planes at $\pm d/2$ becomes

$$\Phi = Ux + Q\chi$$

And the resulting velocity field is found as

$$\nabla\Phi = U + Q \begin{bmatrix} -\frac{x}{r^3} + \int_0^\infty \mu \frac{x}{s} e^{-\mu d} e^{\mu|z|} J_0'(\mu s) d\mu \\ -\frac{y}{r^3} + \int_0^\infty \mu \frac{y}{s} e^{-\mu d} e^{\mu|z|} J_0'(\mu s) d\mu \\ -\frac{z}{r^3} + \int_0^\infty \mu\, sign(z) e^{-\mu d} e^{\mu|z|} J_0(\mu s) d\mu \end{bmatrix}$$

And because $J_0'(\mu s) = -J_1(\mu s)$

$$\begin{aligned} u &= U + Q\left(\frac{x}{r^3} + \int_0^\infty \mu \frac{x}{s} e^{\mu(|z|-d)} J_1(\mu s) d\mu\right) \\ v &= +Q\left(\frac{y}{r^3} + \int_0^\infty \mu \frac{y}{s} e^{\mu(|z|-d)} J_1(\mu s) d\mu\right) \\ w &= +Q\left(\frac{z}{r^3} - \int_0^\infty \mu sign(z) e^{\mu(|z|-d)} J_0(\mu s) d\mu\right) \end{aligned}$$